LA-UR-16-23034
Approved for public release; distribution is unlimited.

Title: Predictive Modeling in Actinide Chemistry and Catalysis

Author(s): Yang, Ping

Intended for: presentation for Chemistry Department at Shannxi Normal University and Shannxi Technological University

Issued: 2016-05-02

Predictive Modeling in Actinide Chemistry and Catalysis

Ping Yang
pyang@lanl.gov

Shannxi Normal University
May 16, 2016 | Xi'an, China

Los Alamos NATIONAL LABORATORY EST.1943

NNSA

Chemical Predictive Modeling

- Modeling and simulation is a critical part of research in science and engineering.
  - Integrated practice of theory and experiment
  - Design new materials and chemistries with predictive power

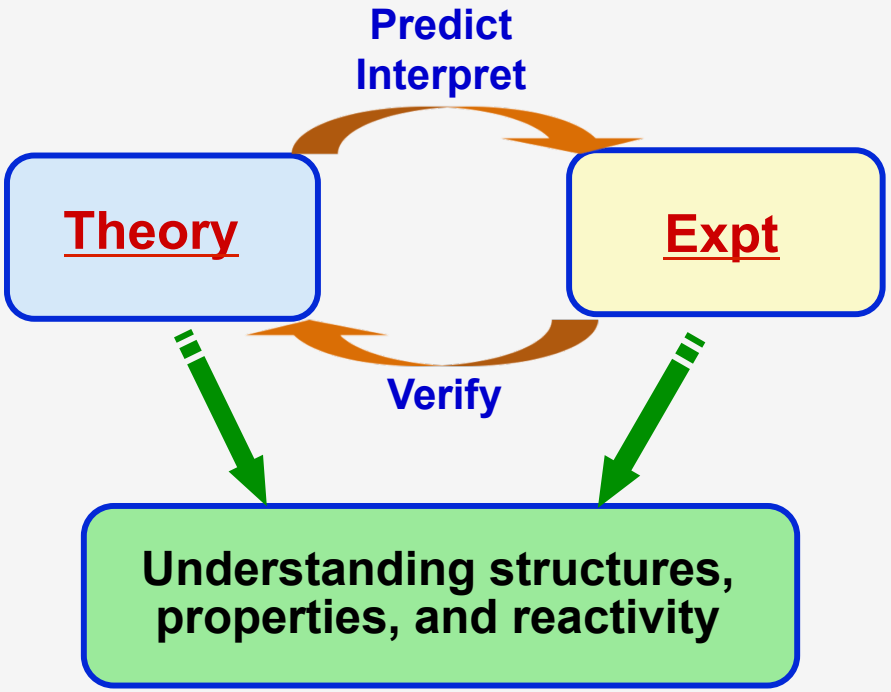

Computational Modeling

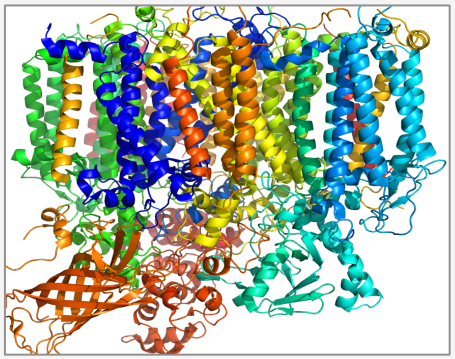

Classical Molecular Mechanics

~1,000,000 atoms

Use empirically-derived potentials

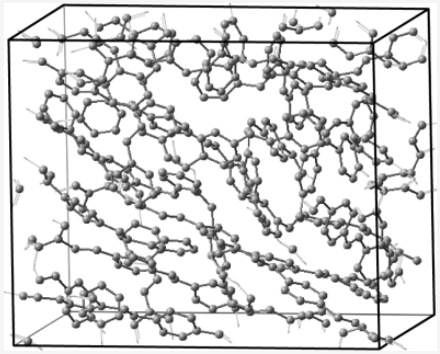

Semi-empirical Quantum Mechanics

~1,000 atoms

Solve approximate Schrödinger equation

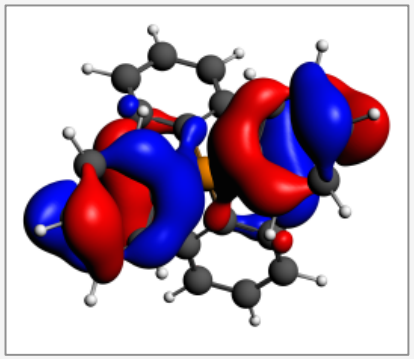

Ab Initio Quantum Mechanics

~200 atoms

Solve Schrödinger equation

Empirical parameters needed

Computationally demanding

Accuracy Needed for Chemical Predictivity

Example: reaction energetics, catalyst design, or separations systems

- Predict equilibrium chemistry: *Selectivity*
  - Change in K_{eq} @ 298 K
  - K_{eq} = 1 50:50 ΔG = 0 kcal/mol
  - K_{eq} = 10 90:10 ΔG = 1.4 kcal/mol
  - K_{eq} = 100 99:1 ΔG = 2.8 kcal/mol

- Predict reaction rates: *Reactivity*
  - Factor of 10 in rate @ 298 K corresponds to a change in E_a of 1.4 kcal /mol

Houk, Cheong, *Nature*, ***455***, *309, 2008*

A Challenging Task

Challenging due to the complexity of systems:

- Computation:
  - Scalar and spin-orbit relativistic effects for heavy elements (Actinides)
  - Correct description of spin distribution on multi-metal centers (catalysis)
  - Proper treatment of the environment: COSMO, QM/MM methods
  - Lack of experimental data for benchmark

- Experiment:
  - Complex system, multiple co-existing species
  - difficult to characterize and identify the structures of individual compounds

Close integration between experiment and theory is the key.

Recent Progress

Recent progress in quantum chemistry and advanced spectroscopic techniques provides increasingly accurate chemical insights for complex systems.

EXPERIMENT	THEORY
◆ Crystal Structures	◆ Relativistic density functional theory
◆ IR spectroscopy	◆ Frequency analysis
◆ Heat of formation	◆ Thermochemistry
◆ Reaction kinetics	◆ Transition state search
◆ UV-Vis, X-ray Absorption Spectroscopy	◆ Time-dependent relativistic DFT
◆ Chemical shifts (NMR)	◆ Spin-orbit NMR calculations
◆ Hyperfine coupling constants	◆ Paramagnetic EPR calculations
◆ Dynamic properties	◆ Molecular dynamics (Ab initio, classical)

Density Functional Theory (DFT)

- DFT is a first-principles method: a very successful approach to describing many-electron systems
- DFT provides an excellent comprise among accuracy, computational cost, and ease of interpretation.
- Features:
  - Quantum mechanical, no system-specific empirical parameters
  - Exchange-correlation functional: LDA,GGA, Meta-GGA, Hybrid, etc
  - Numerically inexpensive (~N^3 cost), computationally allowed for large systems
  - Predict properties in the chemical and material sciences

$$\hat{H}\,\Psi(\mathbf{r}_1,\mathbf{r}_2,\ldots,\mathbf{r}_N) = E\Psi(\mathbf{r}_1,\mathbf{r}_2,\ldots,\mathbf{r}_N)$$

$$E = E[\rho]; \qquad \rho = \sum_{i}^{\mathrm{OCC}} \varphi_i^* \varphi_i$$

$$E[n] = T_S[n] + U_H[n] + E_{XC}[n] + \int d^3r\, v_{ext}(r)\, n(r)$$

Computational Methods

- Broken-symmetry density functional theory (DFT) methods
  - GGA: PBE
  - Hybrid: PBE0
- Relativistic Effects
  - ZORA scalar for geometry optimization
  - ZORA spin-orbit coupling for property analysis
- Basis sets
  - Slater-type, TZ2P for optimization, all-electron for property analysis
- Optical Spectra
  - Time-dependent DFT
- Magnetic resonance properties (NMR/EPR)
  - Second-order properties

Outline

- **Structures, bonding, and reactivity**
  - Bonding can be quantified by optical probes and theory
  - Electronic structures and reaction mechanisms of actinide complexes
- **Magnetic resonance properties**
  - Transition metal catalysts with multi-nuclear centers
  - NMR/EPR parameters
- **Moving to more complex systems**
  - Surface chemistry of nanomaterials
  - Interactions of ligands with nanoparticles
- **Path forward and conclusions**

Outline

- **Structures, bonding, and reactivity**
  - **Bonding can be quantified by optical probes and theory**
  - Electronic structures and reaction mechanisms of actinide complexes
- Magnetic resonance properties
  - Transition metal catalysts with multi-nuclear centers
  - NMR/EPR parameters
- Moving to more complex systems
  - Surface chemistry of nanomaterials
  - Interactions of ligands with nanoparticles
- Path forward and conclusions

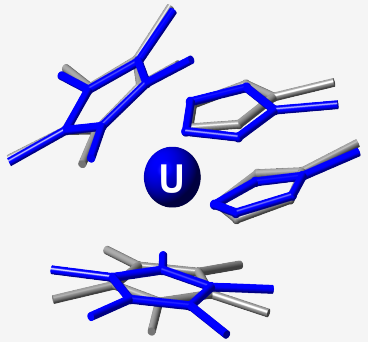

Actinide Chemistry is Important

hydrogen 1 **H** 1.0079												boron 5 **B** 10.811	carbon 6 **C** 12.011	nitrogen 7 **N** 14.007	oxygen 8 **O** 15.999	fluorine 9 **F** 18.998	helium 2 **He** 4.0026
lithium 3 **Li** 6.941	beryllium 4 **Be** 9.0122																neon 10 **Ne** 20.180
sodium 11 **Na** 22.990	magnesium 12 **Mg** 24.305											aluminium 13 **Al** 26.982	silicon 14 **Si** 28.086	phosphorus 15 **P** 30.974	sulfur 16 **S** 32.065	chlorine 17 **Cl** 35.453	argon 18 **Ar** 39.948
potassium 19 **K** 39.098	calcium 20 **Ca** 40.078	scandium 21 **Sc** 44.956	titanium 22 **Ti** 47.867	vanadium 23 **V** 50.942	chromium 24 **Cr** 51.996	manganese 25 **Mn** 54.938	iron 26 **Fe** 55.845	cobalt 27 **Co** 58.933	nickel 28 **Ni** 58.693	copper 29 **Cu** 63.546	zinc 30 **Zn** 65.39	gallium 31 **Ga** 69.723	germanium 32 **Ge** 72.61	arsenic 33 **As** 74.922	selenium 34 **Se** 78.96	bromine 35 **Br** 79.904	krypton 36 **Kr** 83.80
rubidium 37 **Rb** 85.468	strontium 38 **Sr** 87.62	yttrium 39 **Y** 88.906	zirconium 40 **Zr** 91.224	niobium 41 **Nb** 92.906	molybdenum 42 **Mo** 95.94	technetium 43 **Tc** [98]	ruthenium 44 **Ru** 101.07	rhodium 45 **Rh** 102.91	palladium 46 **Pd** 106.42	silver 47 **Ag** 107.87	cadmium 48 **Cd** 112.41	indium 49 **In** 114.82	tin 50 **Sn** 118.71	antimony 51 **Sb** 121.76	tellurium 52 **Te** 127.60	iodine 53 **I** 126.90	xenon 54 **Xe** 131.29
caesium 55 **Cs** 132.91	barium 56 **Ba** 137.33	57-70 *	lutetium 71 **Lu** 174.97	hafnium 72 **Hf** 178.49	tantalum 73 **Ta** 180.95	tungsten 74 **W** 183.84	rhenium 75 **Re** 186.21	osmium 76 **Os** 190.23	iridium 77 **Ir** 192.22	platinum 78 **Pt** 195.08	gold 79 **Au** 196.97	mercury 80 **Hg** 200.59	thallium 81 **Tl** 204.38	lead 82 **Pb** 207.2	bismuth 83 **Bi** 208.98	polonium 84 **Po** [209]	astatine 85 **At** [210]	radon 86 **Rn** [222]
francium 87 **Fr** [223]	radium 88 **Ra** [226]	89-102 **	lawrencium 103 **Lr** [262]	rutherfordium 104 **Rf** [261]	dubnium 105 **Db** [262]	seaborgium 106 **Sg** [266]	bohrium 107 **Bh** [264]	hassium 108 **Hs** [269]	meitnerium 109 **Mt** [268]	ununnilium 110 **Uun** [271]	ununnunium 111 **Uuu** [272]	ununbium 112 **Uub** [277]		ununquadium 114 **Uuq** [289]			

Key: element name / **atomic number** / **symbol** / atomic weight (mean relative mass)

*lanthanoids	lanthanum 57 **La** 138.91	cerium 58 **Ce** 140.12	praseodymium 59 **Pr** 140.91	neodymium 60 **Nd** 144.24	promethium 61 **Pm** [145]	samarium 62 **Sm** 150.36	europium 63 **Eu**	gadolinium 64 **Gd**	terbium 65 **Tb** 158.93	dysprosium 66 **Dy** 162.50	holmium 67 **Ho** 164.93	erbium 68 **Er** 167.26	thulium 69 **Tm** 168.93	ytterbium 70 **Yb** 173.04
**actinoids	89 **Ac**	90 **Th**	91 **Pa**	92 **U**	93 **Np**	94 **Pu**			97 **Bk**	98 **Cf**	99 **Es**	100 **Fm**	101 **Md**	102 **No**

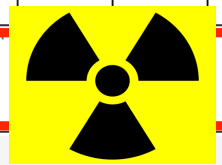

Los Alamos NATIONAL LABORATORY EST.1943

NNSA

Chemical Bonding in Actinide Complexes

- Softer ligands (N- and S-) have significantly improved efficiency.
- Bioremediation is a promising approach to mitigate contamination.
  - Metalloproteins bind to An ions
  - Multiple binding sites with O-, N-, S-coordination
- Bonding of 5f elements has been widely debated:
  - Covalent vs. ionic bonding
  - Involvement of d vs. f orbitals

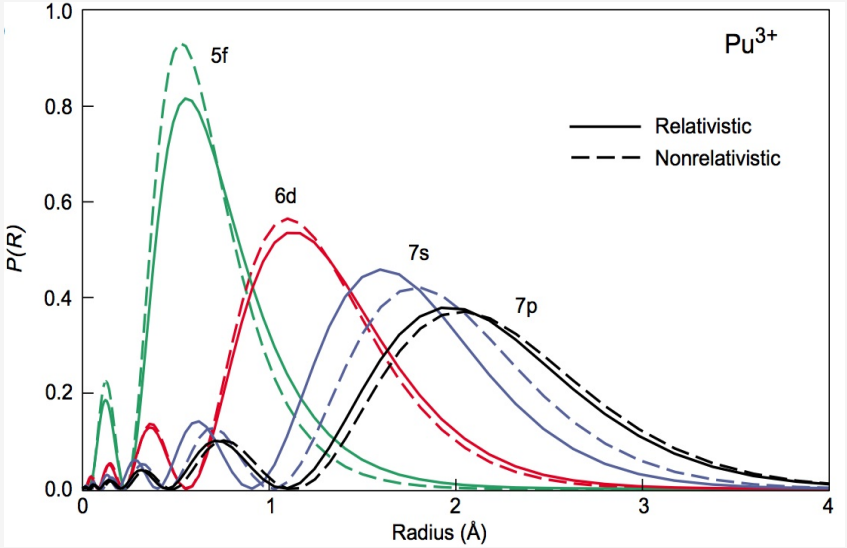

P J Hay, Los Alamos Sci. No 26 Vol II P. 371

R. Denning, *Struct. Bonding*, **1992**, *79*, 215
G. Seaborg, *J. Am. Chem. Soc.* **1954**, *76*, 1461
G. Choppin. *J. Alloys Comp*. **2002**, *344*, 55

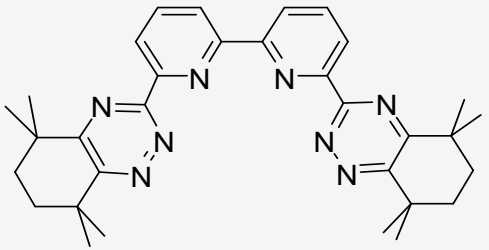

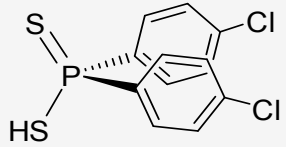

Classical Example: UCl_6^{n-}

- U(VI)→ U(III)
  - Bond length increases
  - Totally stretching frequency decreases
  - U-Cl bonds longer and weaker
- Excellent agreement between optimized structures and X-ray data
- Both 5f and 6d orbital participations is important in U-Cl bonds.

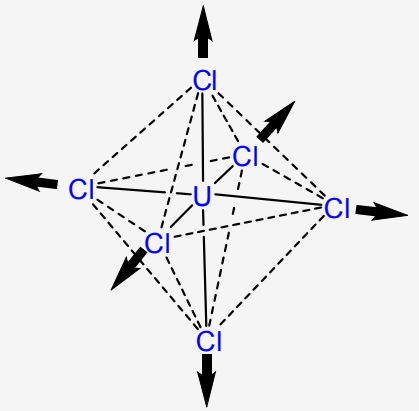

Compd	U-Cl Theory	U-Cl X-ray	ν_1(U-Cl) A_{1g}
UCl_6	2.472	2.42(1)	369
UCl_6^-	2.553	2.513(1)	345
UCl_6^{2-}	2.675	2.626(1)	296
UCl_6^{3-}	2.867	2.803(5)	235

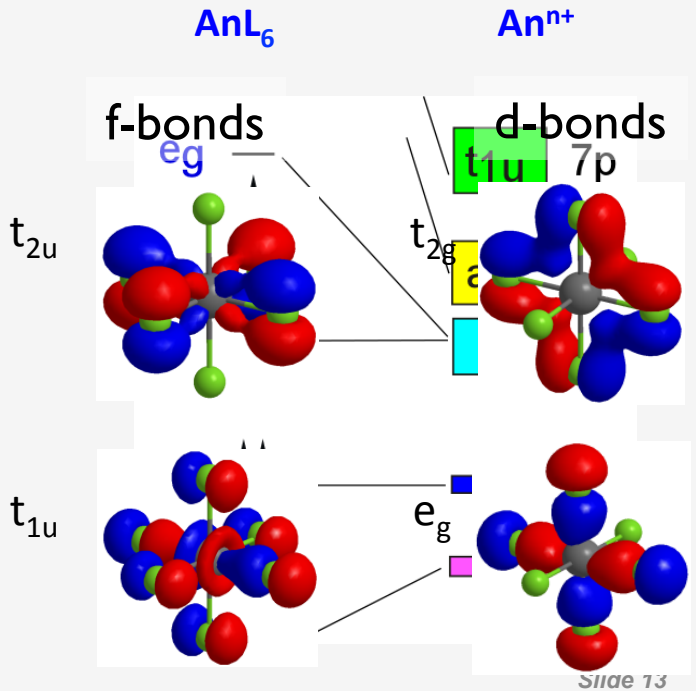

Spectroscopy to Probe Electronic Structures

- Study occupied orbitals
  - Look at orbital mixing
  - Good for computational approaches but not ideal for experimental techniques
- Study virtual orbitals
  - From simulations: anti-bonding coefficients provide information about bonding orbitals
  - From experiments: spectroscopy can probe those states
  - New techniques: Ligand K-edge X-ray Absorption Spectroscopy
- Linear response theory
  - Time-dependent DFT for excited states
  - Oscillator strengths for intensities
  - Only consider core excitations

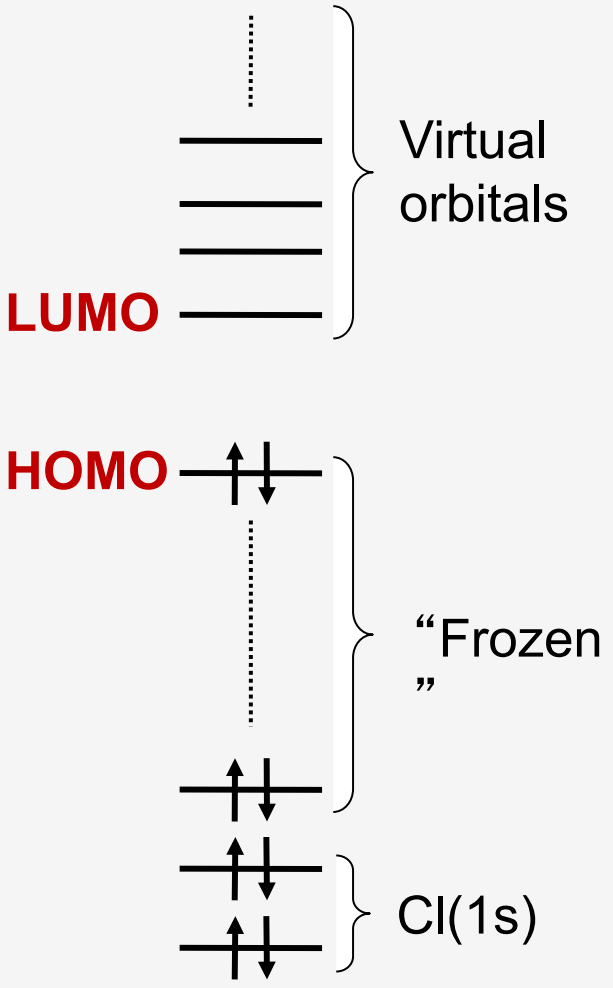

Outline

- Ligand K-edge XAS is a direct, quantitative probe of covalency in M-L bond.
- Dipole absorption $\Delta l = \pm 1$; s → p
- Pre-edge transition intensity derived from L-centered 1*s*->3*p* transition, weighted by c^{*2}_{L}, the covalent character of L 3*p* orbitals in Ψ^*
- Orbital energies provide peak positions and splittings

$$I \propto \langle \Psi_{L(1s)} | r | \Psi^* \rangle$$

Solomon et al., *Coord. Chem. Rev.* **2005**, 249, 97

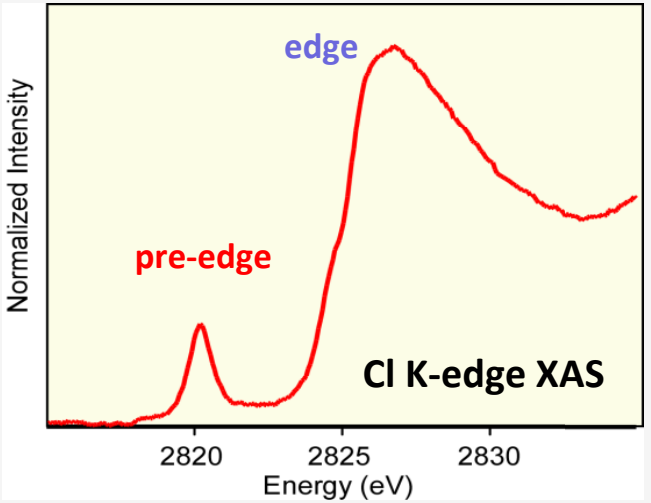

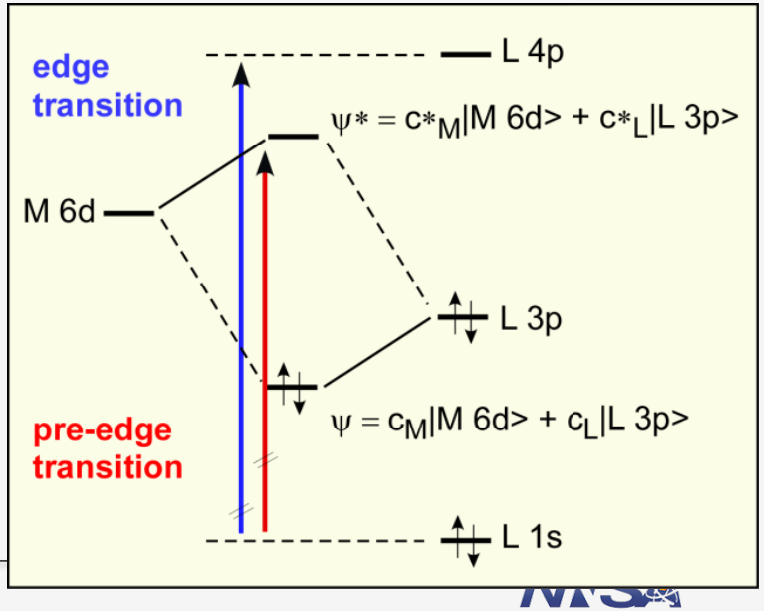

Los Alamos NATIONAL LABORATORY EST.1943

Cl K-edge: WCl_6 (d^0f^0) vs. UCl_6^{1-} (d^0f^1)

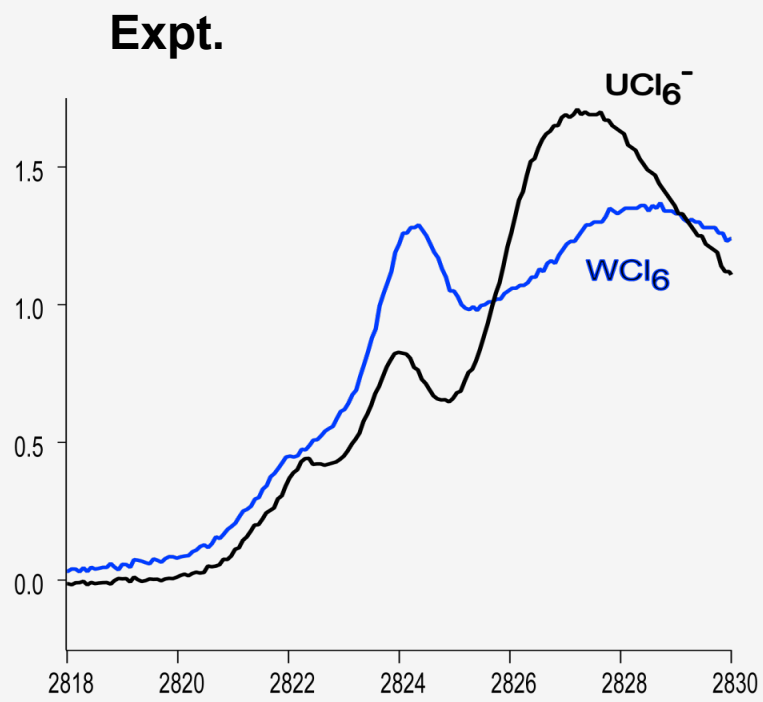

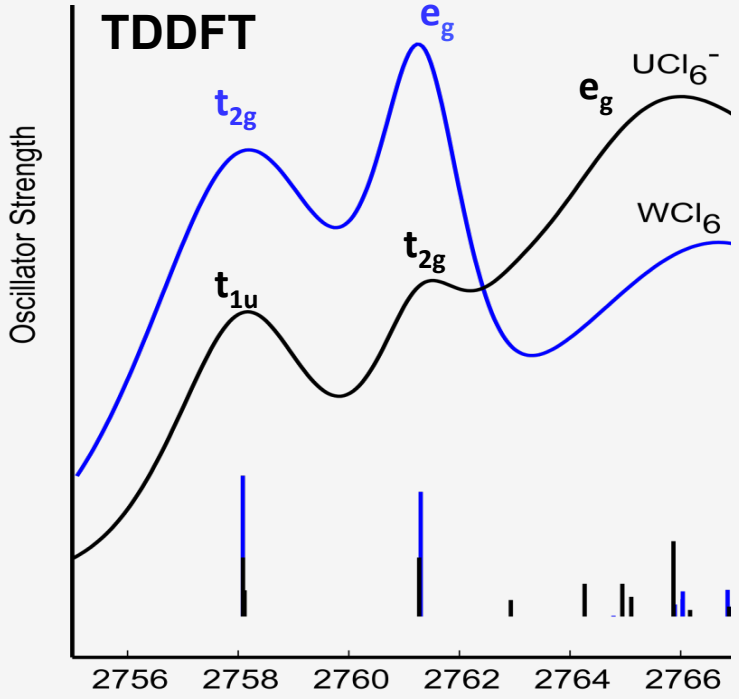

- Transition metal and actinide complexes have peaks at the same positions
- Theory predicts different origin for each peak; d-bands in TM and one f-band and on d-band for actinide complex.
- Direct measure of ligand field splitting (t_{2g}-e_g)

Cl K-edge XAS: TM → Ln → An

$ZrCl_6^{2-}$ **$CeCl_6^{2-}$** **$ThCl_6^{2-}$**

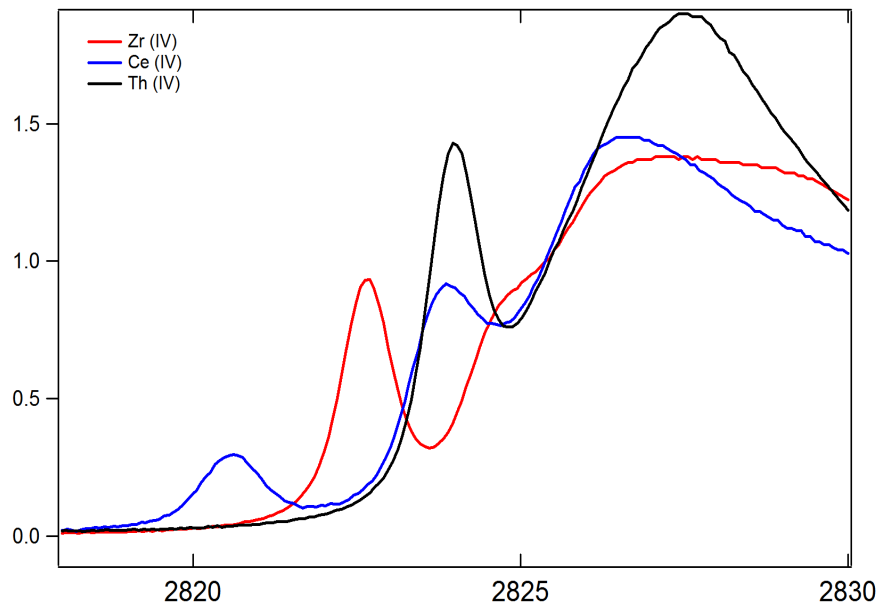

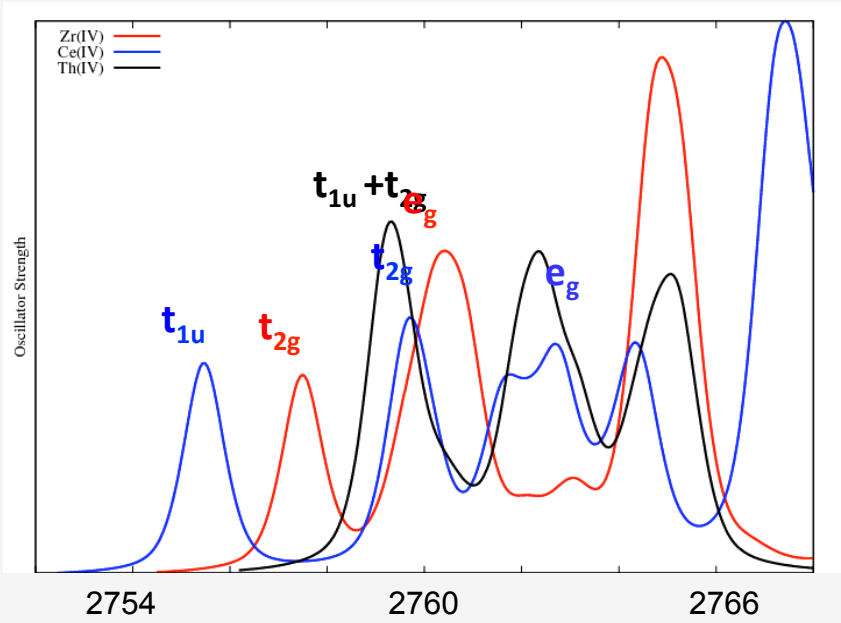

- TM covalency is from d-participation.
- Ce has both 4f- and 5d-manifold.
- Th has mixed 5f- and 6d-contributions (nearly degenerate).

%Cl 3p	Expt.	Theory	
t_{2g}(P1)	--	8.6	$ZrCl_6^{2-}$
e_g(P2)	--	10.1	
t_{1u}(P1)	4.0	7.7	$CeCl_6^{2-}$
t_{2g}(P2)	10.0	7.0	
t_{1u} + t_{2g}	14.5	13.9	$ThCl_6^{2-}$

Los Alamos NATIONAL LABORATORY EST. 1943

Minasian, Yang, et al., *J. Am. Chem. Soc.* **2012** *134,* 5586

NNSA

O K-edge: Covalency in U-O Bond

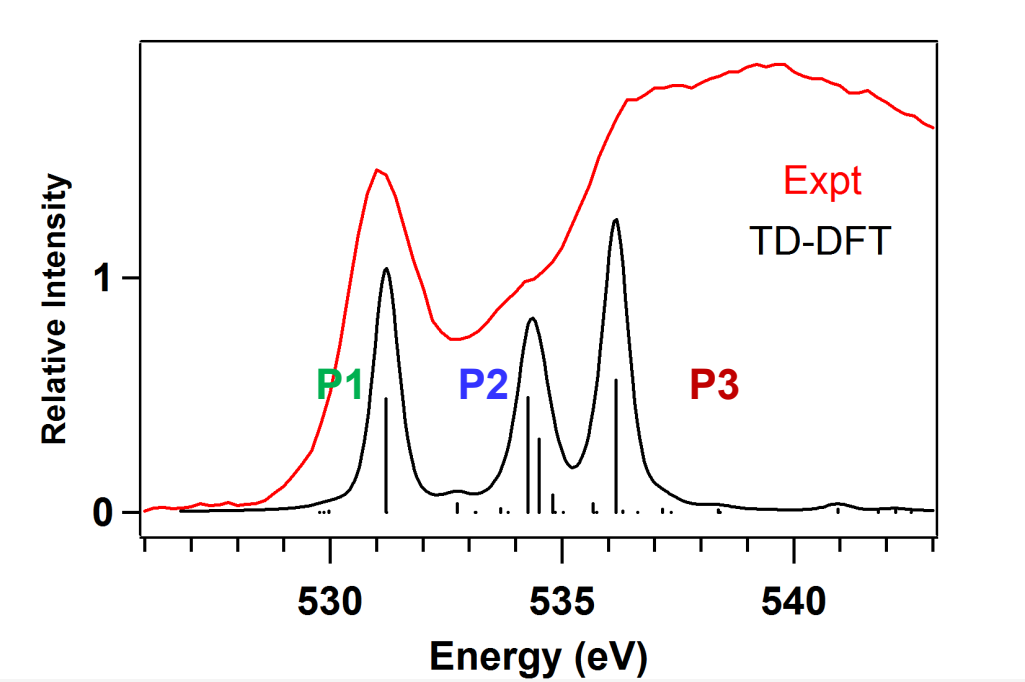

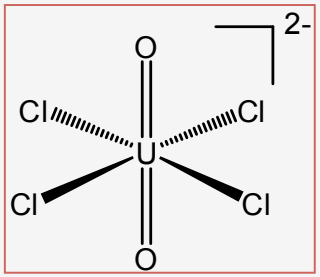

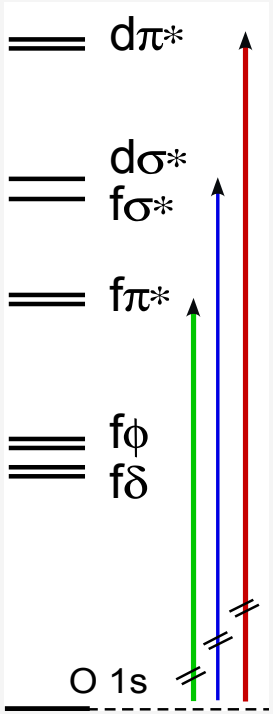

P1 = 73.5% U[5f] + 20.0% O[2p]
P2 = 40.5% U[5f] + 48.2% O[2p]
P3 = 79.5% U[6d] +16.0% O[2p]

Minasian, Yang, et al., *J. Am. Chem. Soc.* **2013**, *135*, 1864

Covalency in U-L Bond

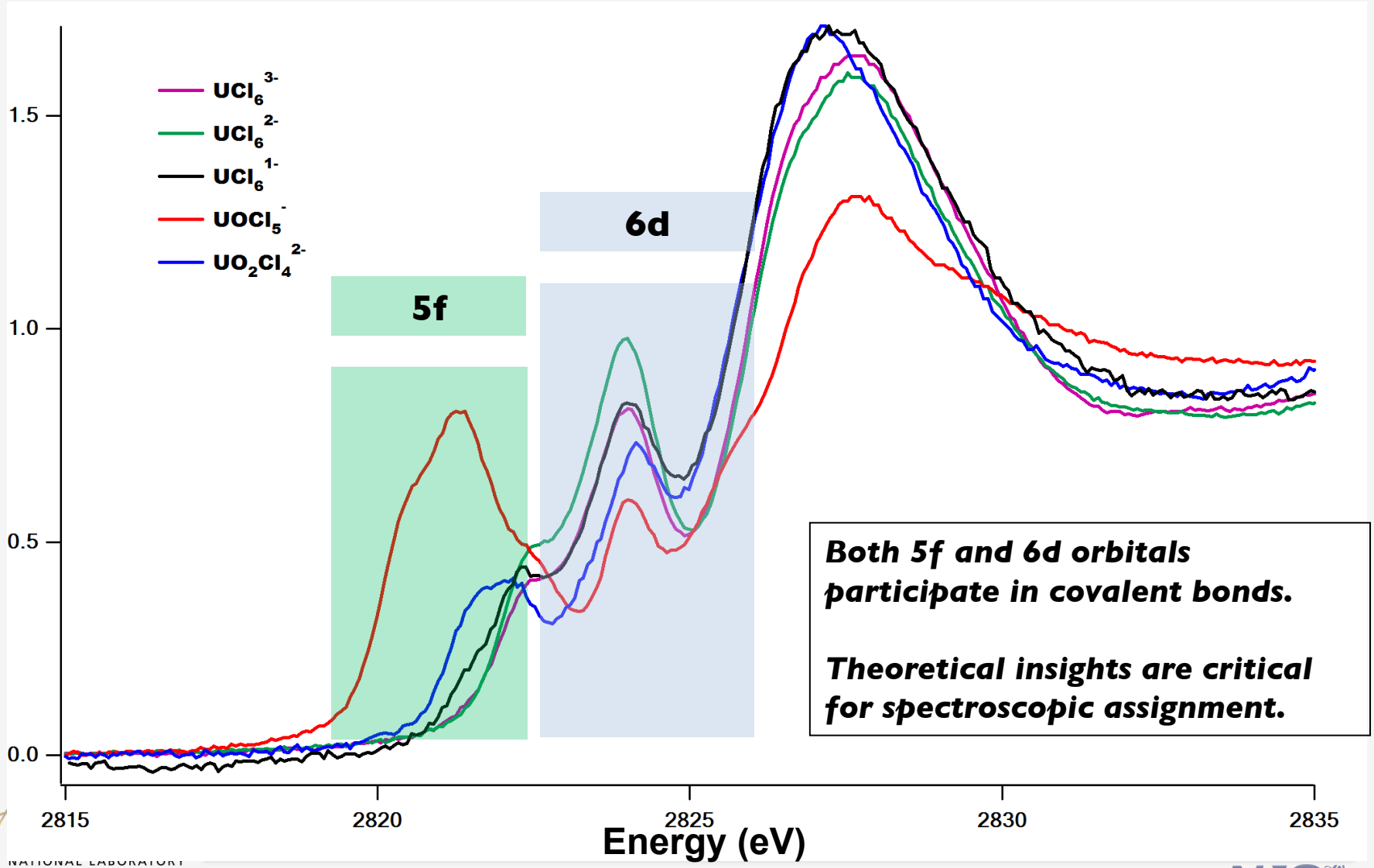

Outline

- **Structures, bonding, and reactivity**
  - Bonding can be quantified by optical probes and theory
  - **Electronic structures and reactivity of complicated actinide complexes**
- Magnetic resonance properties
  - Transition metal catalysts with multi-nuclear centers
  - NMR/EPR parameters
- Moving to more complex systems
  - Surface chemistry of nanomaterials
  - Interactions of ligands with nanoparticles
- Path forward and conclusions

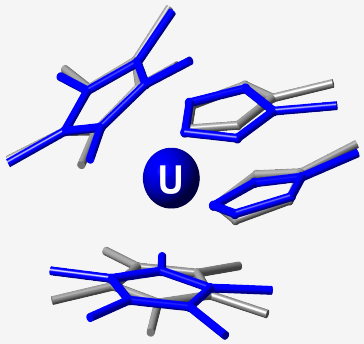

Electronic Structures of N-rich Actinide Complexes

- Metal complexes with nitrogen-rich ligand present unique chemical and physical properties, including
  - Nonlinear optical materials, metal-organic frameworks, and luminescent materials, etc.
- However, chemistry of N-rich complexes of actinide is unexplored.

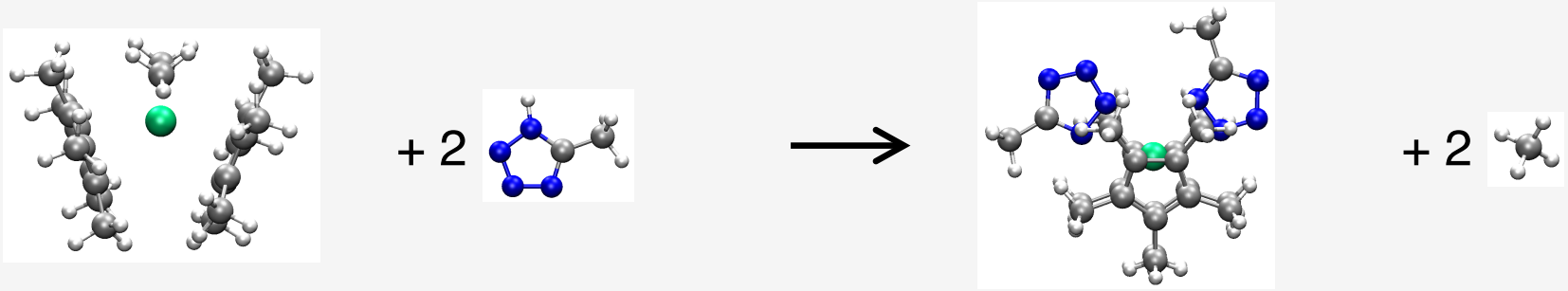

$Cp^*_2An(CH_3)_2$ + 2 methyl tetrazole ⟶ $Cp^*_2An(tetrazolate)_2$ + 2 CH_4

ΔG = –375 kJ/mol (U)
–383 kJ/mol (Th)

Los Alamos NATIONAL LABORATORY EST. 1943

Browne, Maerzke, et al. *Inorg Chem.* 2016, ASAP

NNSA

$Cp^*_2An(tet)_2$ Structure

- Excellent agreement between the calculated and crystal structures
  - 3% error in metal-ligand bond lengths
  - 7% error in bond angles

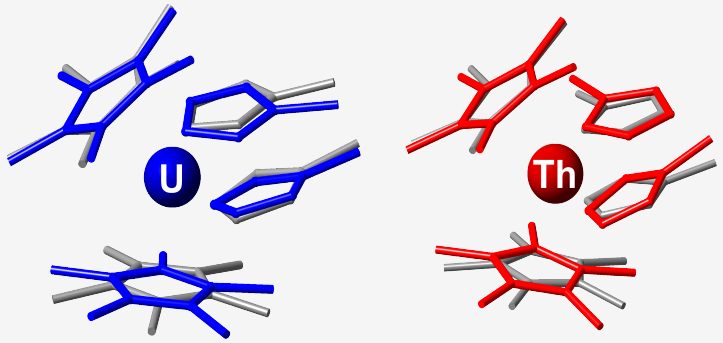

crystal structures (grey) and calculated structures (blue, red)

- Note the different orientations of the tetrazolate methyl groups

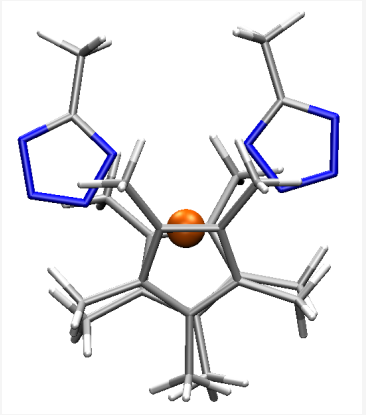

U

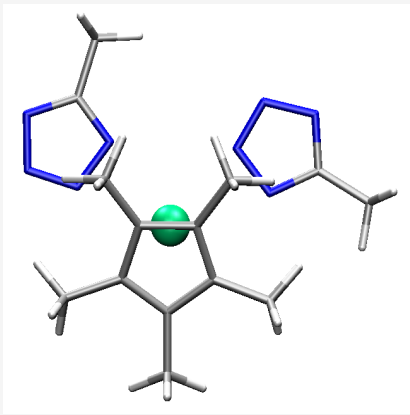

Th

Los Alamos NATIONAL LABORATORY EST.1943

Browne, Maerzke, et al. *Inorg Chem.* 2016, ASAP

NNSA

$Cp^*_2An(tet)_2$ Tetrazolate Orientations

- Crystal structures corresponding configurations with lowest free energy.
- A and B have very small free energies difference. They might coexist in solution.
- Proton chemical shift of the methyl group will be diagnostic.
  - Calculated $\delta_A - \delta_B = 0.12$ ppm
- dynamic equilibrium between A and B confirmed by variable-temperature NMR experiments on $Cp^*_2Th(tet)_2$
  - Experimental measurement $\delta_A - \delta_B = 0.16$ ppm

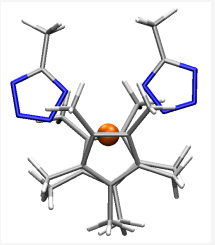

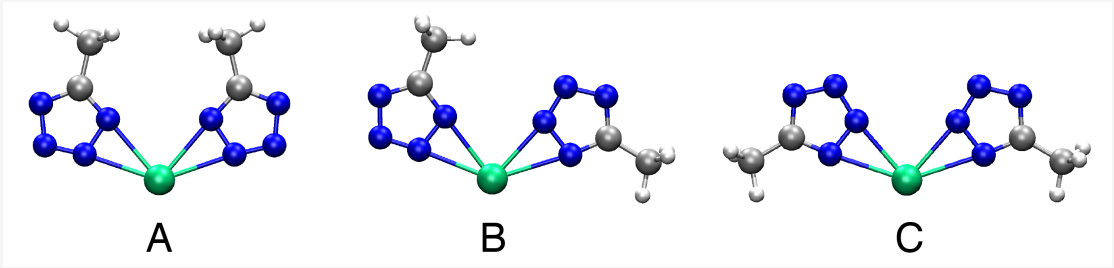

	ΔG [kJ/mol]	
	U	**Th**
A	**0.0**	6.5
B	7.1	**0.0**
C	22.0	19.0

Los Alamos NATIONAL LABORATORY EST. 1943

Browne, Maerzke, et al. *Inorg Chem.* 2016, ASAP

NNSA

Molecular Orbital Diagram

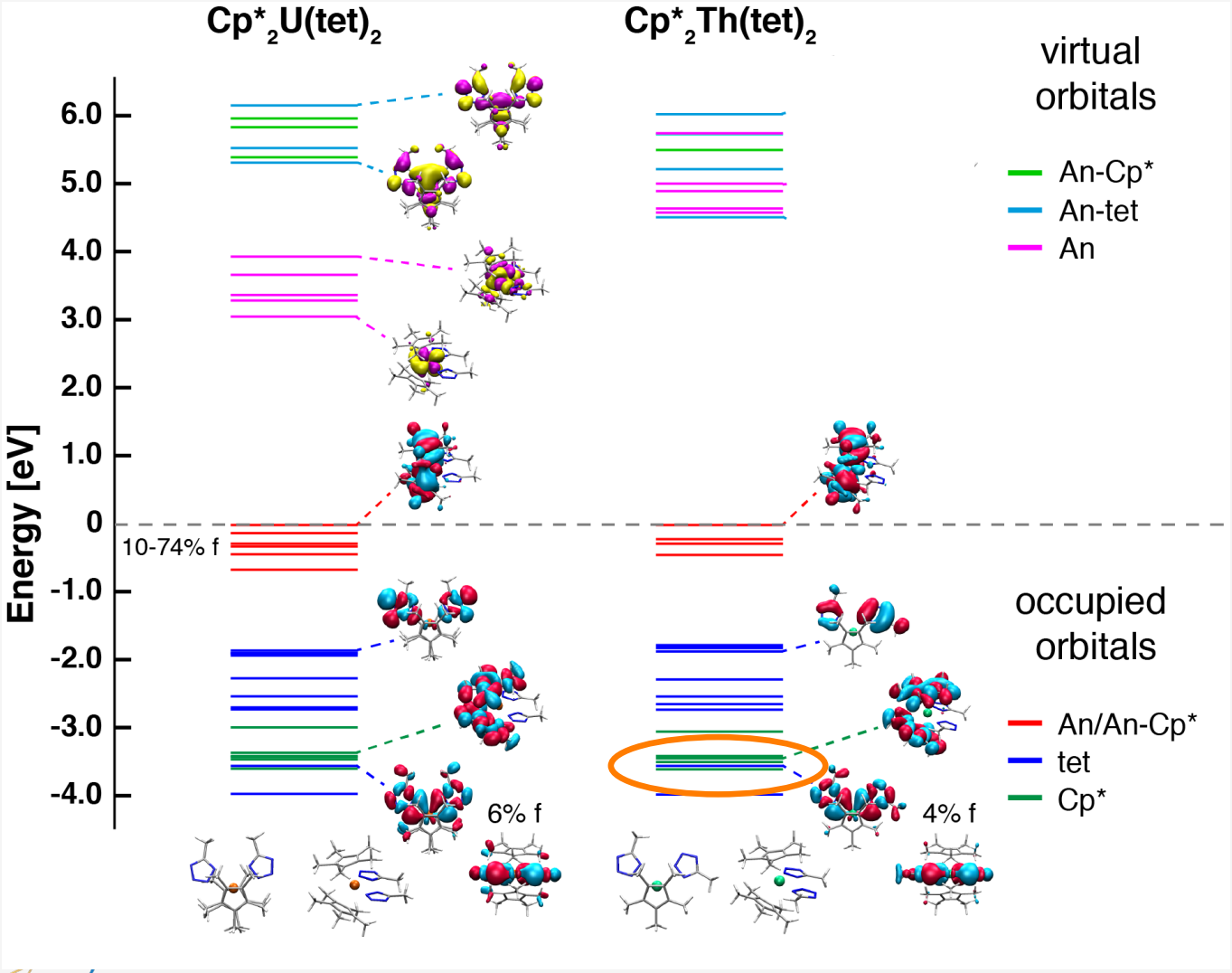

- Frontier orbitals dominated by metal-Cp* bonding interactions
- Orbitals N-rich ligand buried deep
- Small overlap between An-tet
- Mainly ionic interactions between An-tet

Browne, Maerzke, et al. *Inorg Chem.* 2016, ASAP

Electronic Spectroscopy

- Good agreement between experimental UV-Vis spectra and TD-DFT calculations.

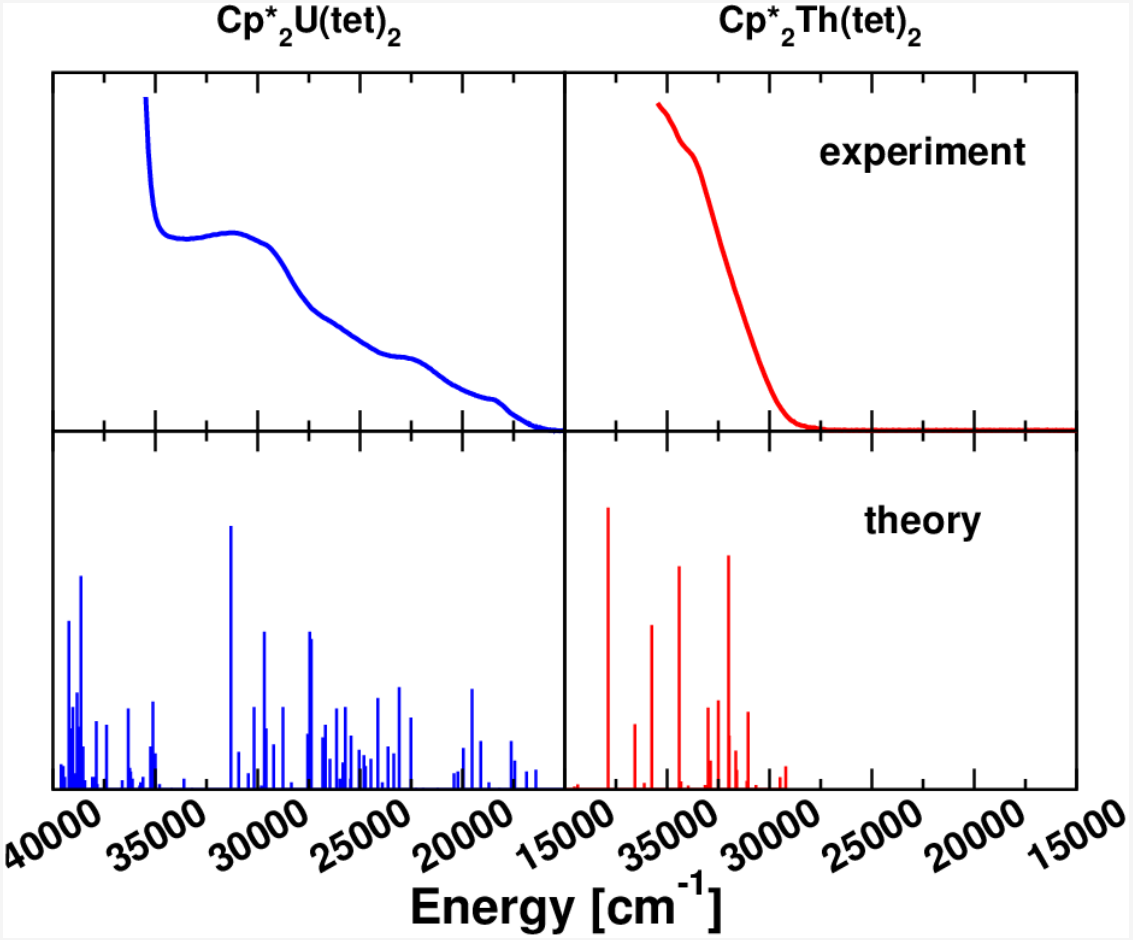

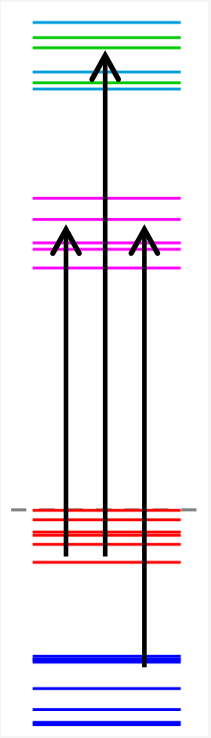

Los Alamos NATIONAL LABORATORY EST.1943

Browne, Maerzke, et al. *Inorg Chem.* 2016, ASAP

NNSA

Outline

- Structures, bonding, and reactivity
  - Actinide chemistry
  - Geometric Structures, thermochemistry, and reaction mechanisms
- **Magnetic resonance properties**
  - **Transition metal catalysts with multi-nuclear centers**
  - **NMR/EPR parameters**
- Moving to larger systems
  - Surface chemistry of nanomaterials
  - Interactions of ligands with nanoparticles
- Path forward and conclusions

Complexes Relevant to Catalysis

- Catalysis is one of the most efficient and important methods to facilitate chemical transformations.
- Electronic structures determine catalytic properties; this can be monitored with magnetic probes.

  - Dinuclear metalloradicals with direct metal-metal bonding
    - Functional metal-containing polymers
    - EPR for paramagnetic systems

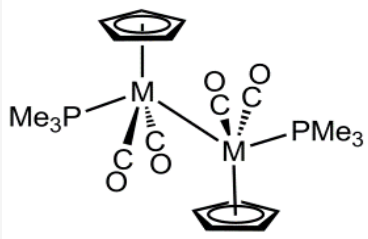

  - Dinuclear metal complexes with bridging ligands
    - Catalytic centers in metalloproteins: PSII, hydrogenanses
    - Metal center cryogenic NMR

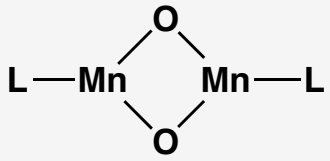

Theory Background for NMR/EPR Calculations

- Nuclear shielding (chemical shift):

$$\sigma_A = E^{(m_A,B)} = \left.\frac{\partial^2 E}{\partial m_A \partial B}\right|_{\substack{m_A=0 \\ B=0}} \qquad \delta \approx \sigma_{\text{ref}} - \sigma_{\text{sample}}$$

- Electric Field Gradients (EFG):

$$G_{\alpha\beta}(\mathbf{r}) = \int \mathrm{d}^3 r \frac{n(\mathbf{r})}{|\mathbf{r} - \mathbf{r}'|^3}\left[\delta_{\alpha\beta} - 3\frac{(r_\alpha - r_\alpha')(r_\beta - r_\beta')}{|\mathbf{r} - \mathbf{r}'|^2}\right]$$

- Quadrupolar coupling constant, C_Q, for nuclear spin $I > 1/2$:

$$C_Q = \frac{eV_{zz}Q}{h} \qquad \text{Where, } |V_{zz}| > |V_{yy}| > |V_{xx}|$$

- Electron paramagnetic resonance (EPR) parameter, *g*-tensors:

$$g_{uv} = \frac{1}{\beta_e}\frac{\partial^2 E}{\partial B_u \partial S_v}$$

First Unsupported Metal-Metal Radical

- Group 6 dimers have direct M-M single bonds.
  - Electrochemistry underscores the need for bridging ligands in stabilizing odd electron dimers.

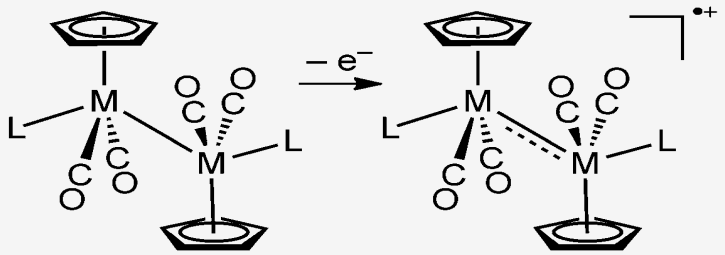

M = Mo, W; L=CO
M = Mo; L= $PPyPh_2$

Adams RD, DM Collins, FA Cotton, *Inorg. Chem.* 1974, 13:1086

- Success with stronger donor phosphane ligands

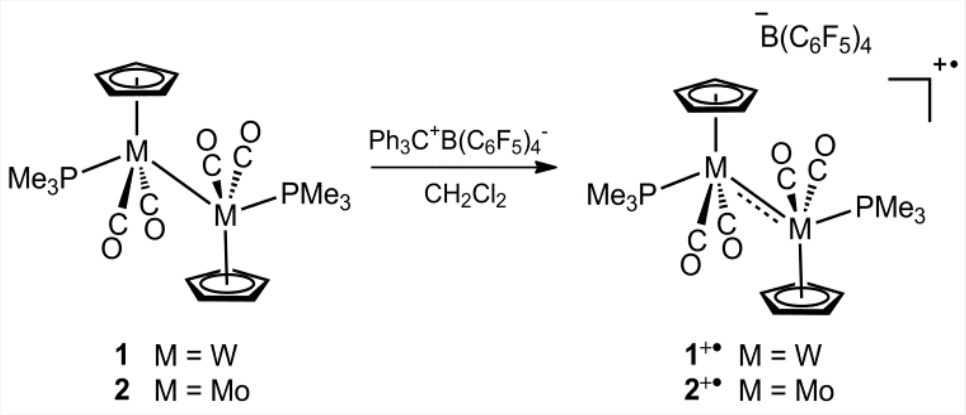

Los Alamos NATIONAL LABORATORY EST. 1943

NNSA

First Unsupported Metal-Metal Radical

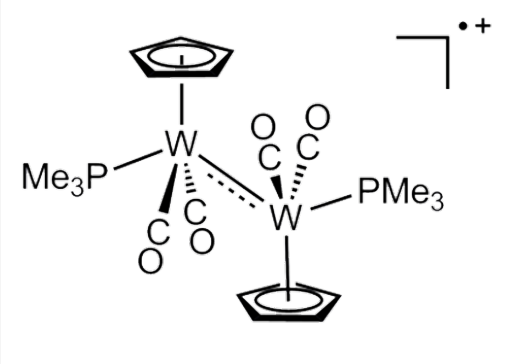

W-W bond length		
	expt	DFT
1	3.233	3.335
1^{+*}	3.026	3.127

- **Removal of one electron from HOMO, a W-W antibonding π orbital, increases bond order to 1½**

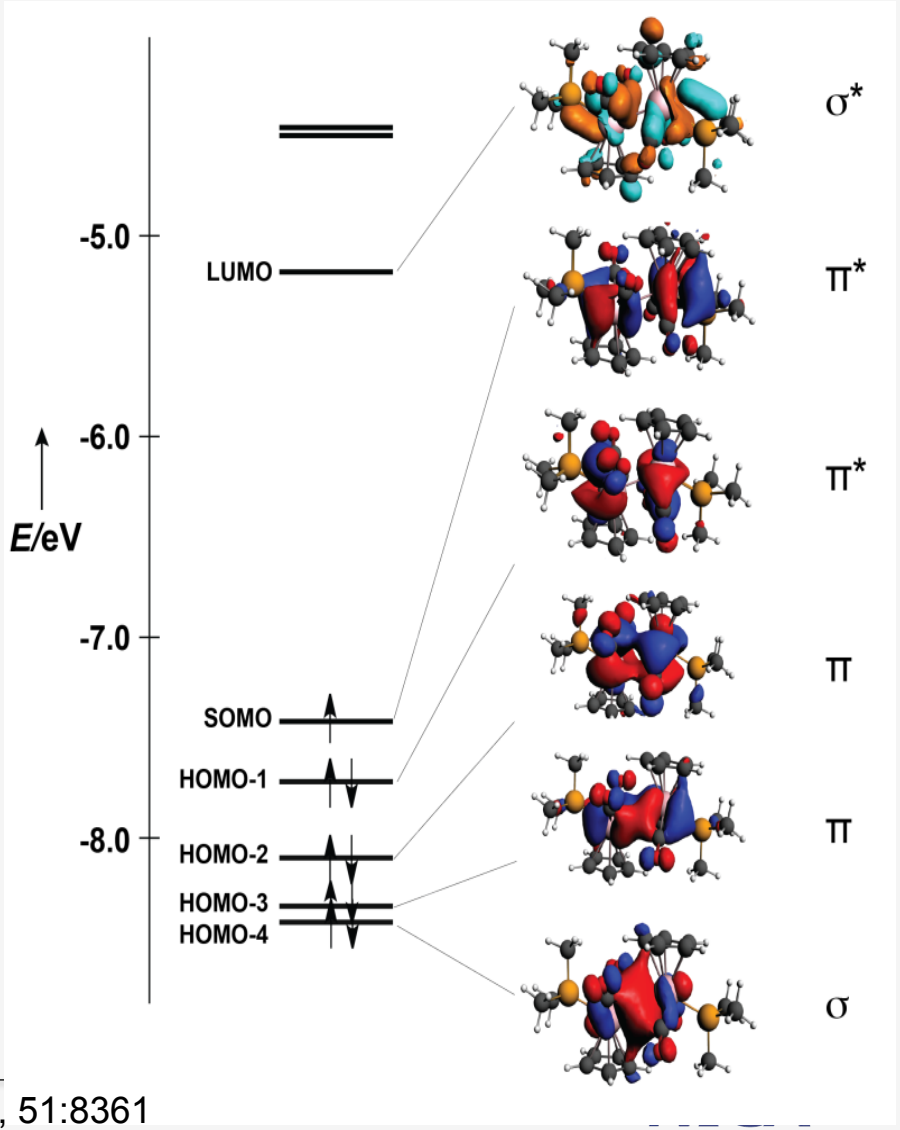

Los Alamos NATIONAL LABORATORY

van der Eide, Yang, et al. *Angew Chem Int. Ed.* 2012, 51:8361

Metal-Metal Bonding and Spectroscopy

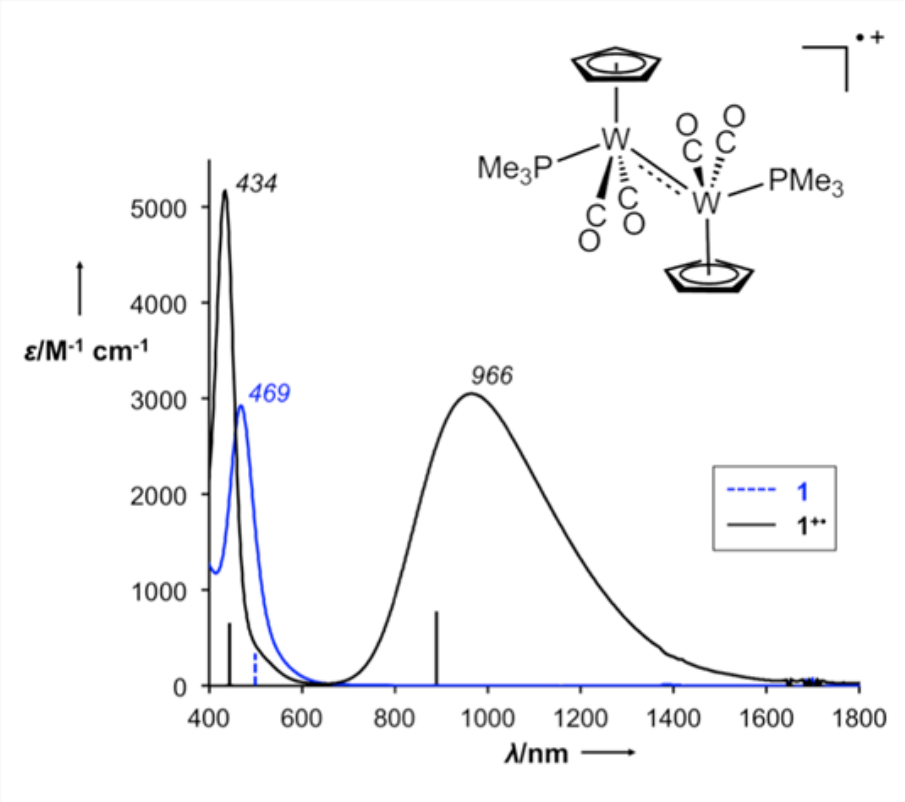

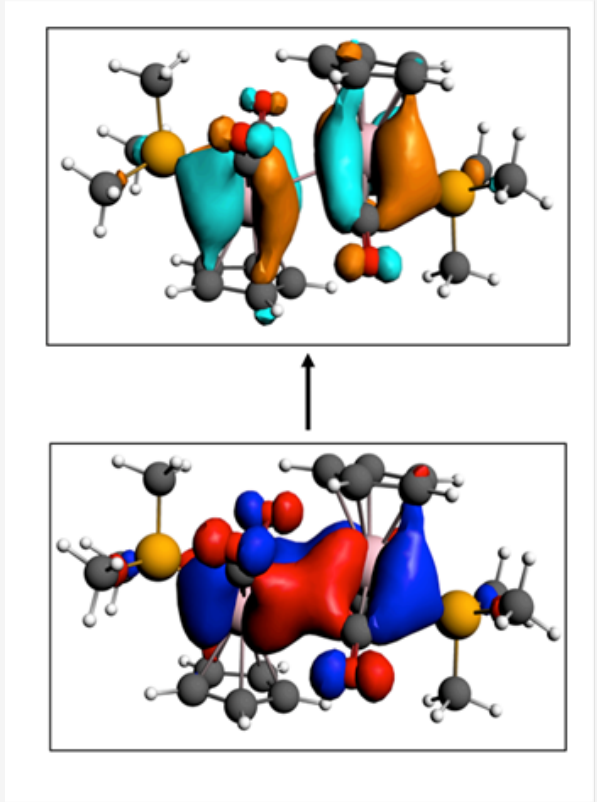

- TD-DFT assigned the NIR adsorption at 966nm to a $\pi \rightarrow \pi^*$ transition, HOMO-3 → SOMO.
- Mo-Mo complex has NIR absorption at λ_{max}=1110nm.

Los Alamos NATIONAL LABORATORY EST.1943

van der Eide, Yang, et al. *Angew Chem Int. Ed.* 2012, 51:8361

NNSA

EPR Spectroscopy

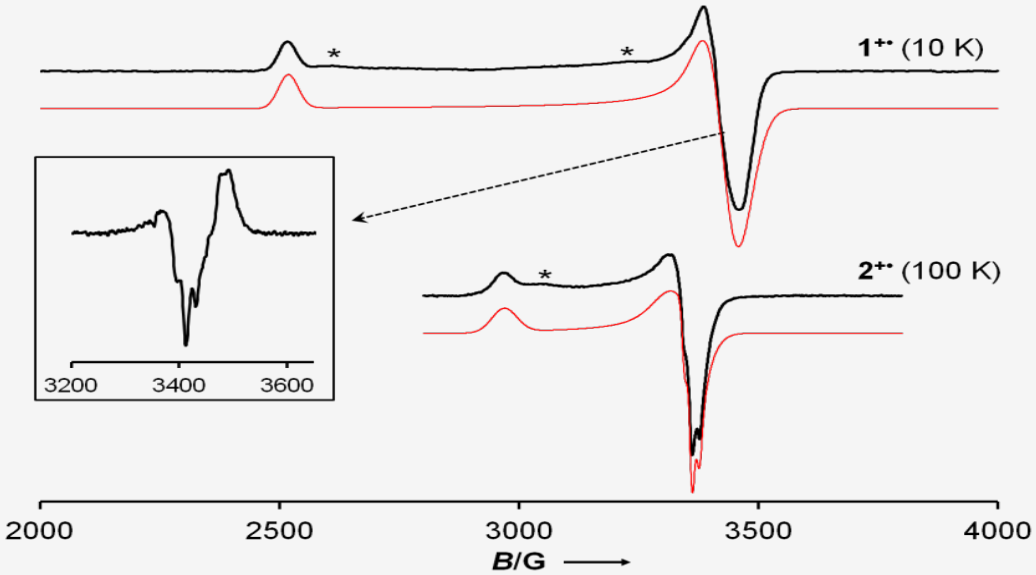

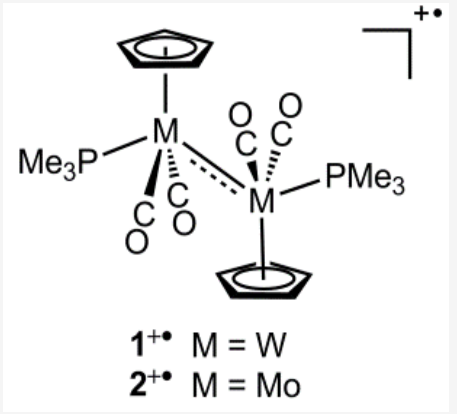

EPR Parameters			
	g_1	g_2	g_3
1^{+*} (expt)	2.664	1.955	1.940
1^{+*} (DFT)	2.606	1.988	1.954

EPR Parameters			
	g_1	g_2	g_3
2^{+*} (expt)	2.258	2.002	1.996
2^{+*} (DFT)	2.229	2.005	1.996

Los Alamos NATIONAL LABORATORY EST.1943

van der Eide, Yang, et al. *Angew Chem Int. Ed.* 2012, 51:8361

NNSA

Bridged Metal Dimer: Mn_2(IV,IV)

Structure

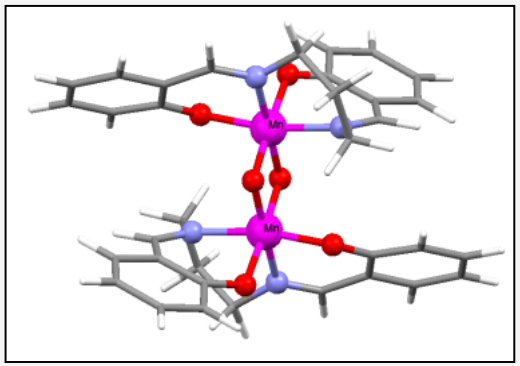

Anti-ferromagnetic coupling

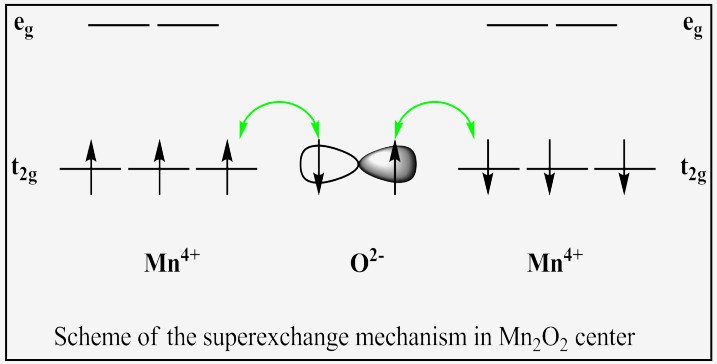

Scheme of the superexchange mechanism in Mn_2O_2 center

Bonding Orbital

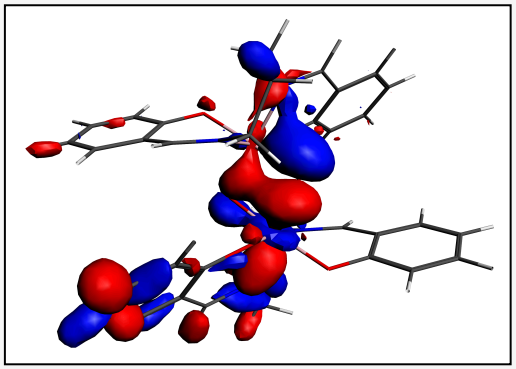

Calculated geometry and crystal structure of $Mn_2O_2(salpn)_2$ are in excellent agreement.

Ground state is an antiferromagnetically coupled singlet state (S=0) and the high spin state is found to be 4.4 kcal/mol higher in energy.

Los Alamos NATIONAL LABORATORY EST.1943

Ellis, Yang, et al. *J. Am. Chem. Soc, 2010,* ***132****:16767*

NNSA

Cryogenic NMR of Mn_2(IV,IV)

First solid-state NMR of an antiferromagnetic complex (S=0)

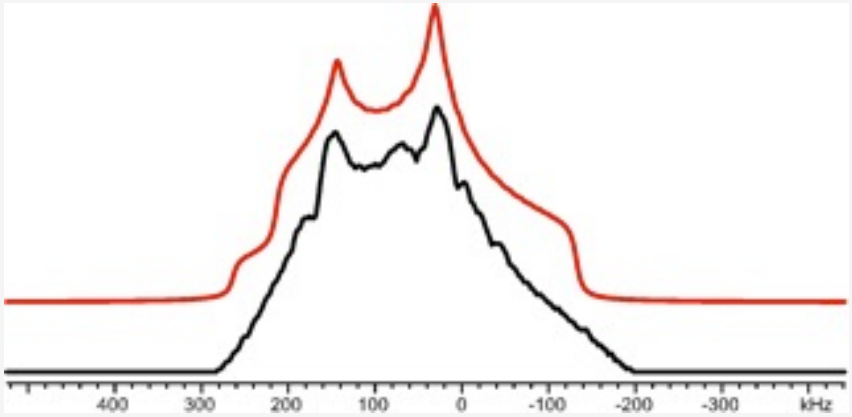

Solid-state ^{55}Mn NMR collected at 9.4 T/ 8.5 K

Measurements require low temperature.

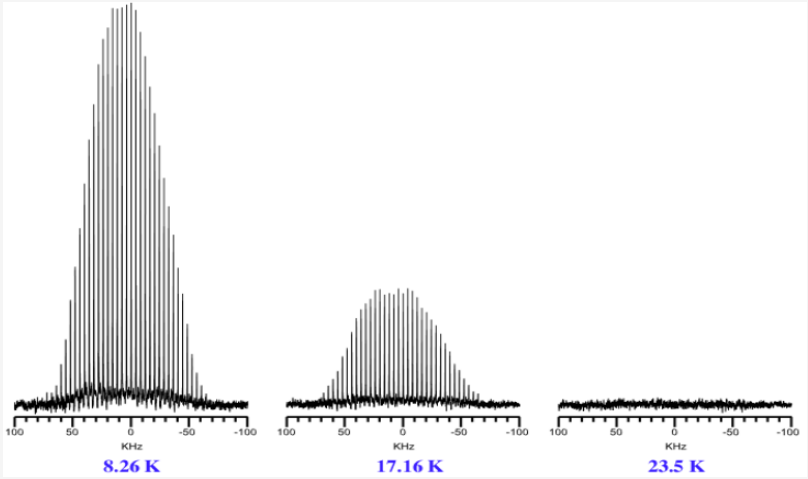

Temperature dependence of the on-resonance portion of the ^{55}Mn spectrum acquired at 9.4 T

- **Highly sensitive, spectrum above results from only 7 mg of material**
- **Require J≤ -40 cm^{-1} for appreciable signal intensity**

	C_Q(MHz)	J (cm^{-1})
Expt.	24.7	-92
Calc.	23.4	-128

Los Alamos NATIONAL LABORATORY EST.1943

Ellis, Yang, et al. *J. Am. Chem. Soc, 2010,* ***132****:16767*

NNSA

NMR is a Sensitive Probe

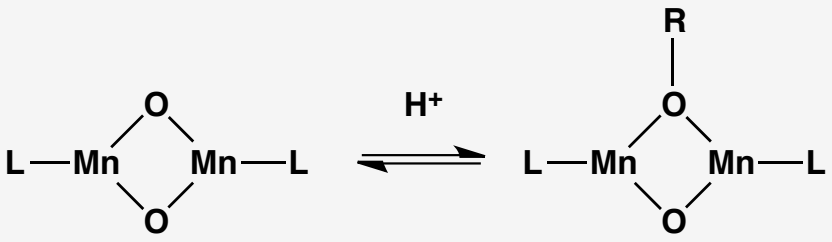

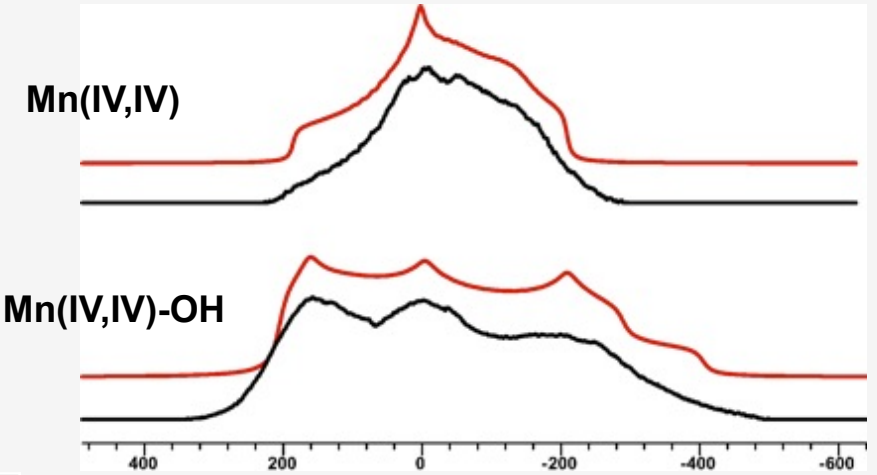

Expt. Calc.	$[MnLO]_2$	$[Mn_2L_2(O,OH)]^+$
J (cm^{-1})	-92 -128.2	-48 -70.4
C_Q(MHz)	26.4 23.4	33.7 23.2 / 40.9
Mn-Mn (Å)	2.73 2.722	2.83 2.877
Mn-O (Å)	1.816/1.821 1.828/1.850	1.828/1.817
Mn-O(H) (Å)		1.972/1.988

- NMR parameters, EFG and exchange coupling J value are sensitive probes of structures.
- All-electron basis sets are required.
- Finite size nucleus for nuclear model, Gaussian improves the results.

Unpublished data, by Lipton at PNNL

Outline

- Structures, bonding, and reactivity
  - Actinide complexes
  - Electronic structures, optical properties, and reaction mechanisms
- Magnetic resonance properties
  - Transition metal catalysts with multi-nuclear centers
  - NMR/EPR parameters
- **Moving to more complex systems**
  - **Surface chemistry of nanomaterials**
  - **Interactions of ligands with nanoparticles**
- Path forward and conclusions

Roles of Capping Ligands

- Stabilize structural and optoelectronic properties
- Insulating/protecting nanoparticles (NPs)
- Adjust solubility of NPs
- Anchor points for chemical/biological functional groups
- Nanotoxicity

Motivations:

- Structural-properties relationship
- Design of functional ligands

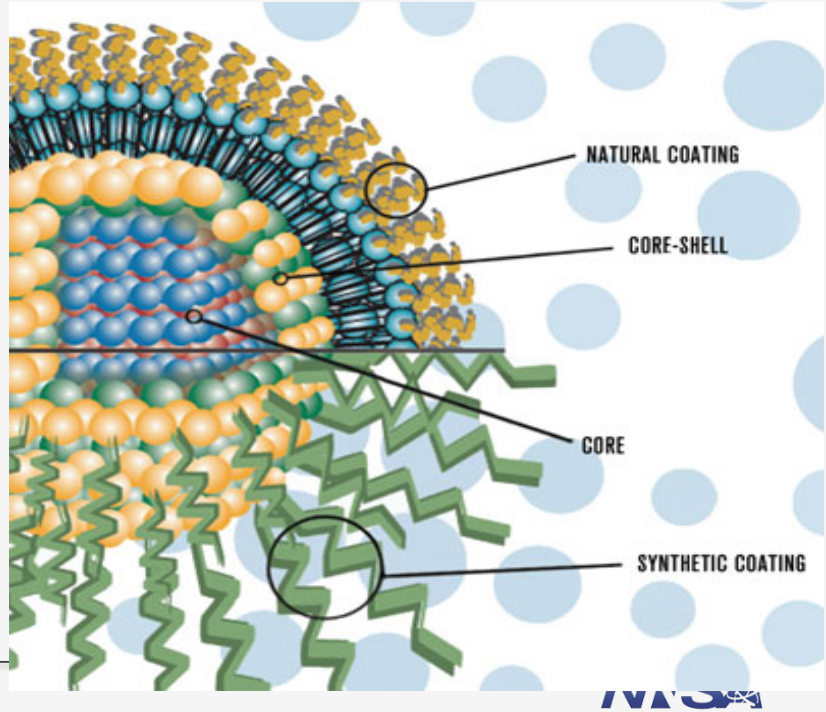

Nanoceria System

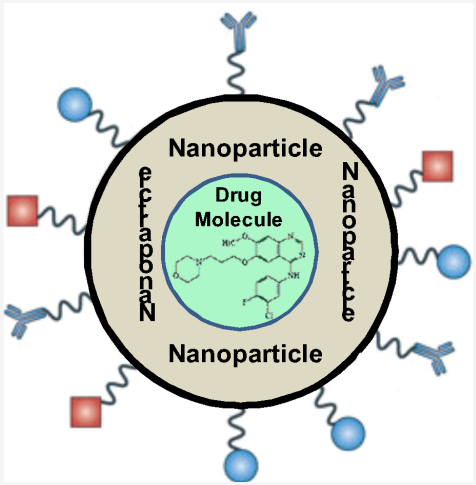

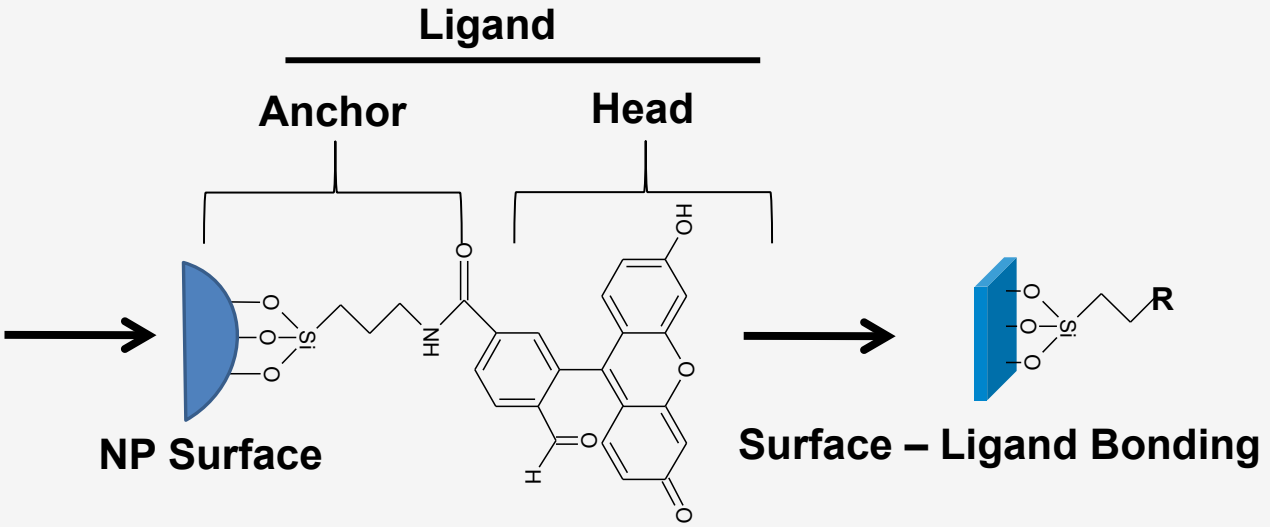

Surface – Ligand Interaction is of paramount importance!

Carboxylic acid as anchors

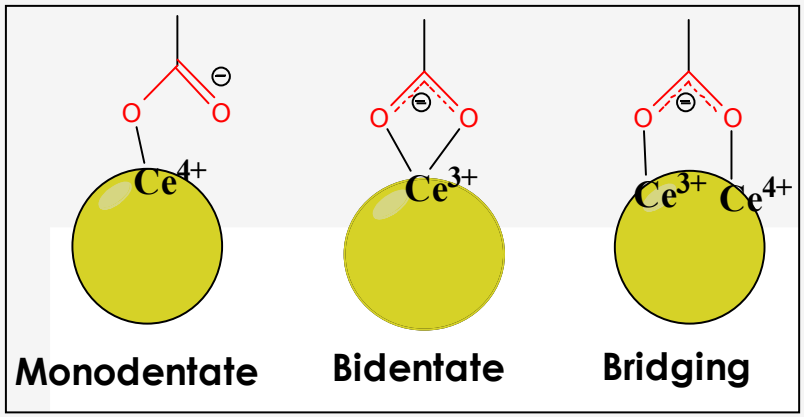

Carboxylic Acids on Nanoceria

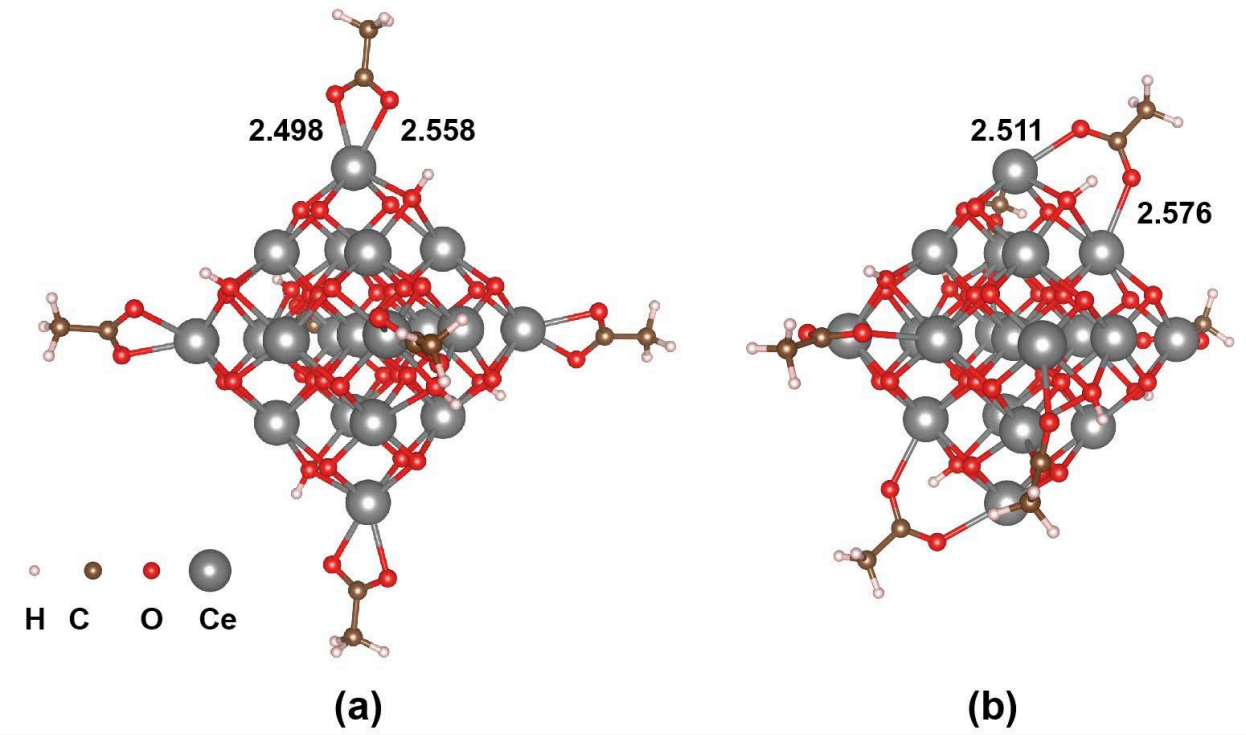

BE per ligand	**-47.2 kcal/mol**	**-43.9 kcal/mol**
s.s. $-CO_2^-$ mode	**1450 cm^{-1}**	**1430 cm^{-1}**

Experimental Verification – SFG-VS Spectra

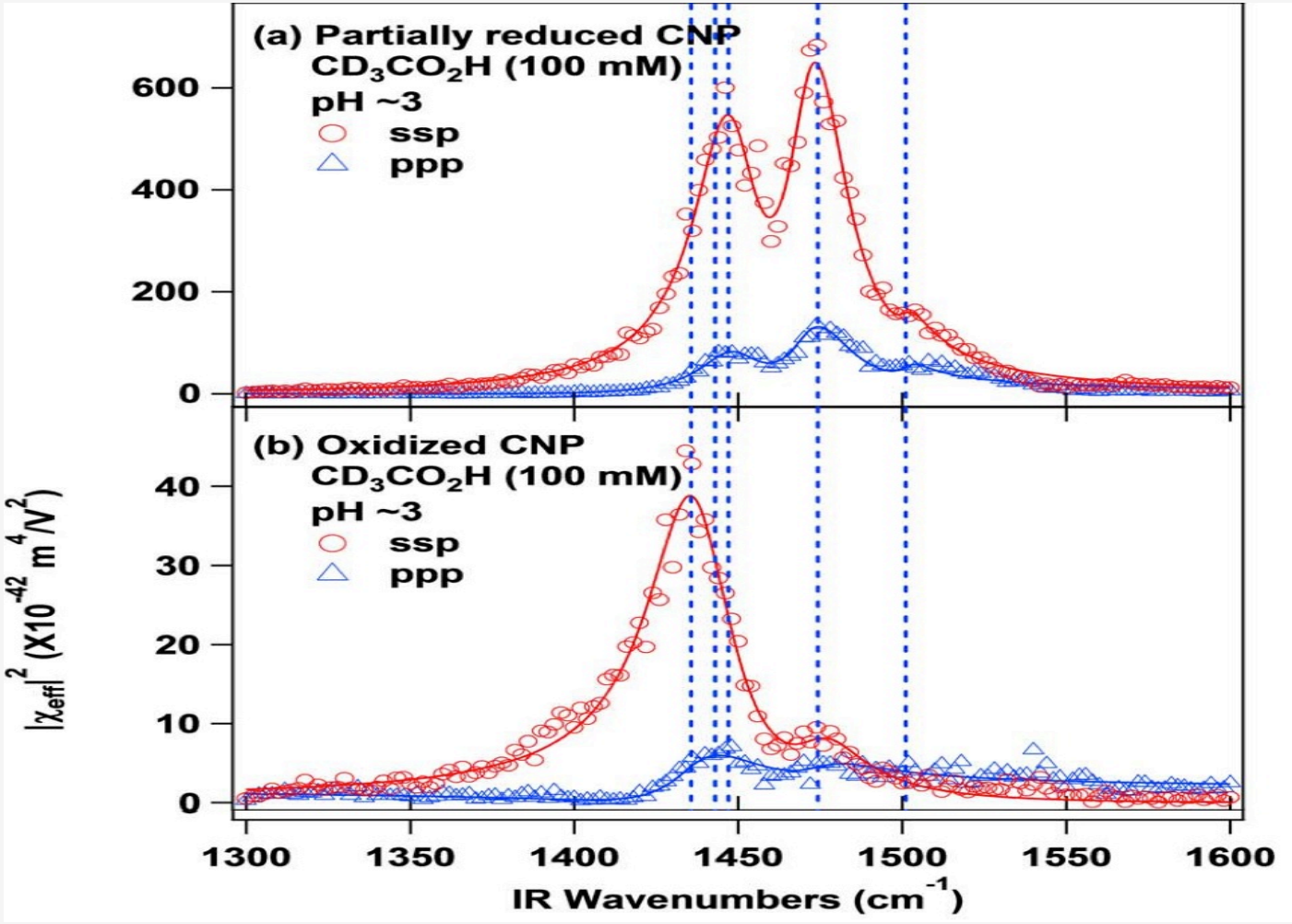

Los Alamos NATIONAL LABORATORY EST.1943

*Lu, Yang, et al, J. Phys. Chem C 2013, **117**:24329*

NNSA

Path Forward

- Computational design is ready to take its place as an essential component of chemistry and material design
  - Predictive power
  - Explains chemical phenomena
  - Provides information inaccessible to experiments, e.g. TS, Actinides
  - Predicts properties and reactivity, subsequently verified by experiments
  - Especially important for the systems that are difficult to synthesize

- Great opportunities to predictively design energy conversion materials and nanomaterials containing transition metals and heavy elements

Acknowledgements

Morris Bullock
EF Van der Eide
Andrew Lipton
Eric Walter
Hongfei Wang

Stosh A. Kozimor
Enrique R. Batista
Kevin Browne
Katie Maerzke
Neil Henson
Jackie Kiplinger
Jackie Veauthier

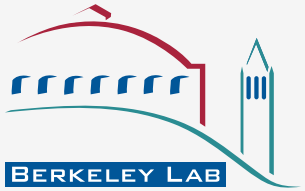

Stephen Minasian
David K Shuh
John Gibson

Funding: LANL LDRD Projects

Thank you !

Shannxi Normal University
May 16, 2016 | Xi'an, China

Los Alamos NATIONAL LABORATORY EST.1943

NNSA

Thank you !

Shannxi Normal University
May 16, 2016 | Xi'an, China

Los Alamos NATIONAL LABORATORY EST.1943

NNSA

Approaches: Uniting Theory and Experiments

- Computational Methods
  - Density functional theory
    - PBE
  - Relativistic effects
    - Scalar broken-symmetry ZORA for structures and energies
  - Basis sets
    - TZ2P Slater-type basis sets
    - BSSE correction for binding energies is included
- Gas-phase Experiments
  - Electrospray ionization (ESI) source with quadrupole ion trap mass spectrometry (QIT/MS)
  - Fragmentation by collision induced dissociation (CID)

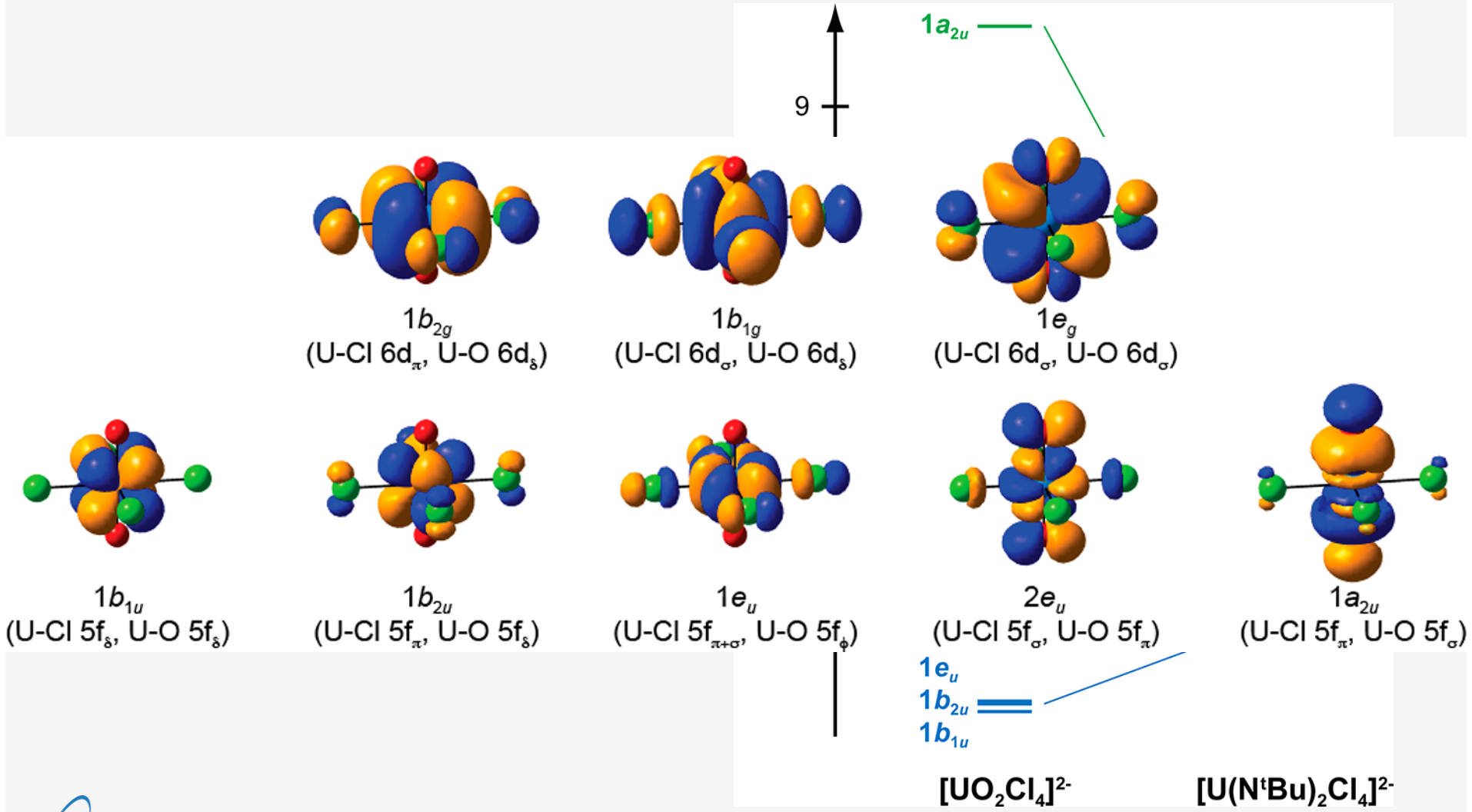

Los Alamos NATIONAL LABORATORY EST.1943

NNSA

Bonding Interactions of Uranium Complexes

UO_2^{2+} $U(NR)_2^{2+}$

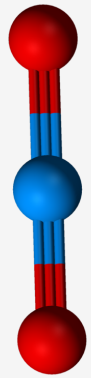

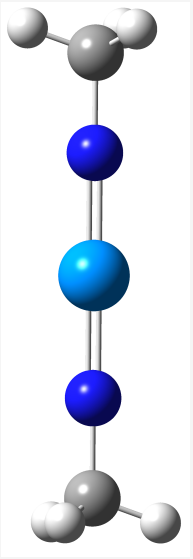

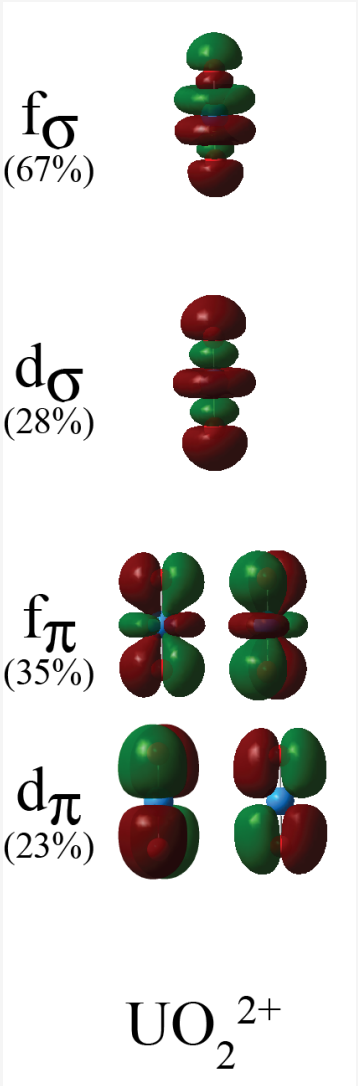

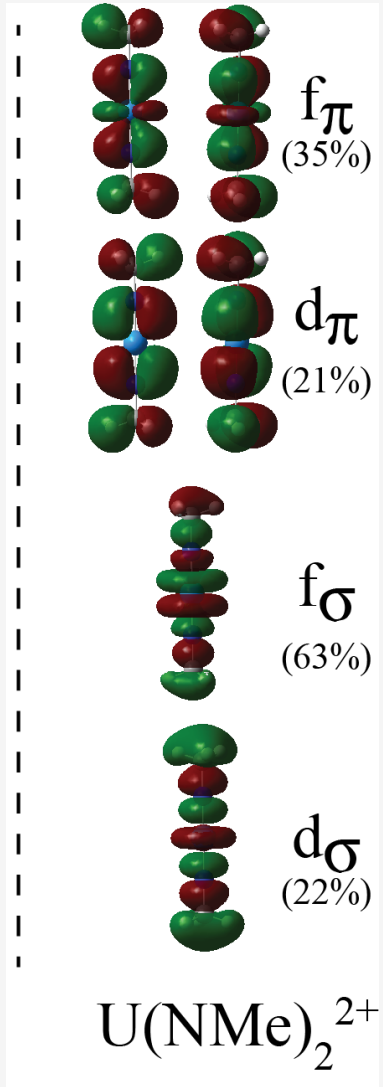

Denning, *J. Phys Chem A* **2007**, *111*: 4125

Hayton, et al *Science* **2005**, *310*: 1941

Batista, Martin, Yang, **2015,** Computational Methods in Lanthanide and Actinide Chemistry, Wiley

Cl K-edge: $UO_2Cl_4^{2-}$ vs. $U(NR)_2Cl_4^{2-}$

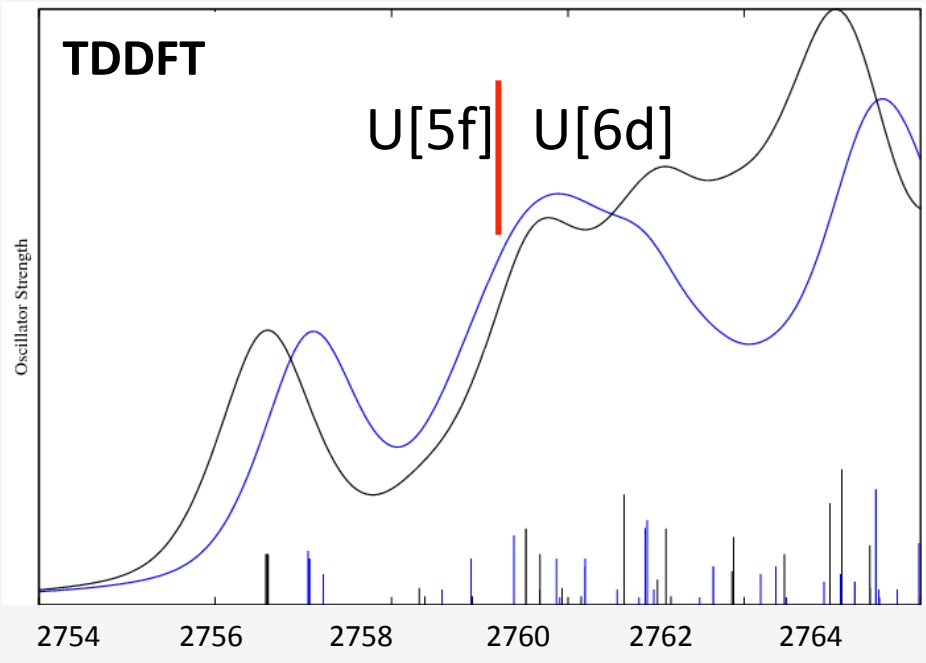

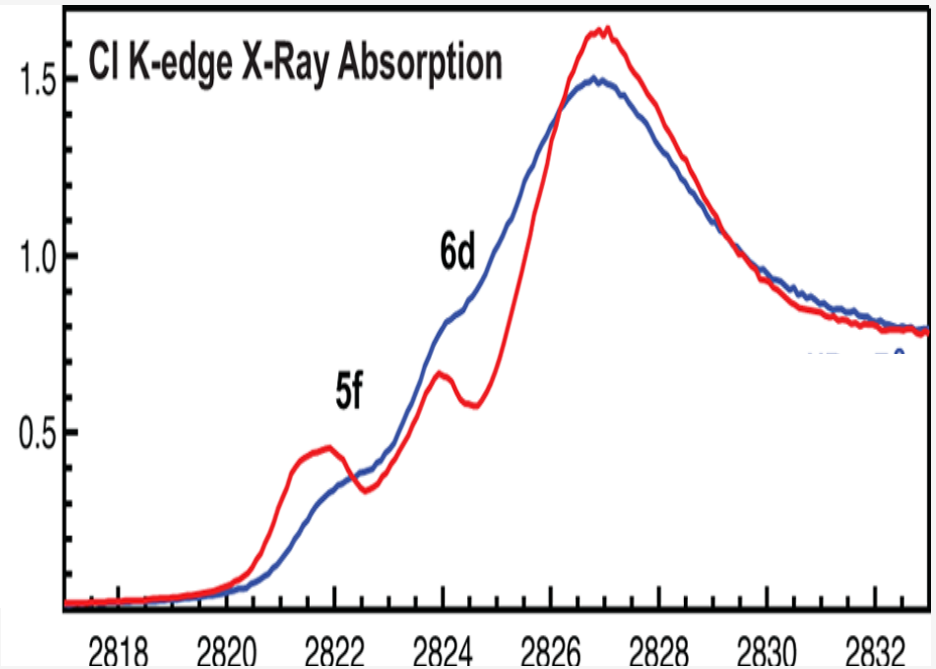

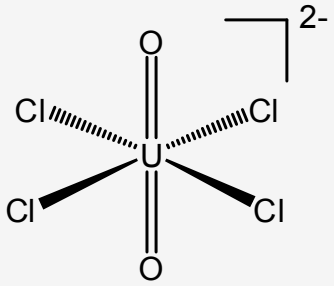

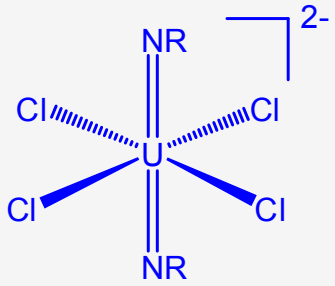

- Little effects on covalency of U-Cl bonds moving from oxo to imido
- Significantly reduced U-Cl mixing (~10%) compared to UCl_6 (~30%) due to two highly covalent U-O and U-N bonds.

Spencer, Yang, et al, *J. Am. Chem. Soc*, ***135***, *2279, 2013*

Equatorial U-E Bond (E=O, S, Se, Te, Po)

- Excellent agreement between theoretical structures and experimental findings. Bond lengths < 3%; angles < 9%.

- Covalent interactions in the U-E bond increase as the size of chalcogenate donor increases. Both 5f and 6d orbital participations is important in U-E bonds.

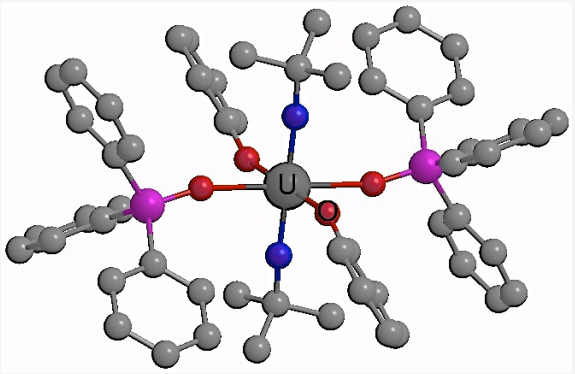

	experimental geometry				at optimized geometry			
E	U−E−C_{ipso} (deg)	U−E (Å)	U−$OPPh_3$ (Å)	U=N (Å)	U−E−C_{ipso} (deg)	U−E (Å)	U−$OPPh_3$ (Å)	U=N (Å)
O	145.06	2.267	2.341	1.870	149.9	2.261	2.451	1.875
S	109.98	2.757	2.322	1.840	119.2	2.791	2.433	1.862
Se	106.43	2.887	2.360	1.861	115.2	2.933	2.431	1.860
Te	103.90	3.092	2.366	1.863	111.8	3.184	2.428	1.857
Po	*a*	*a*	*a*	*a*	111.1	3.252	2.427	1.856

Spencer, Yang, et al, *Inorganic Chemistry*, ***48***, *2693, 2009*

Reaction Mechanism: Imido Exchange

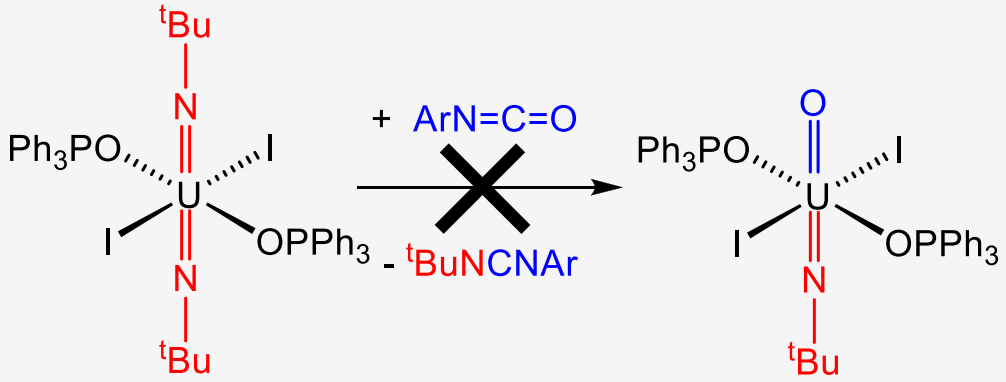

1 **2**

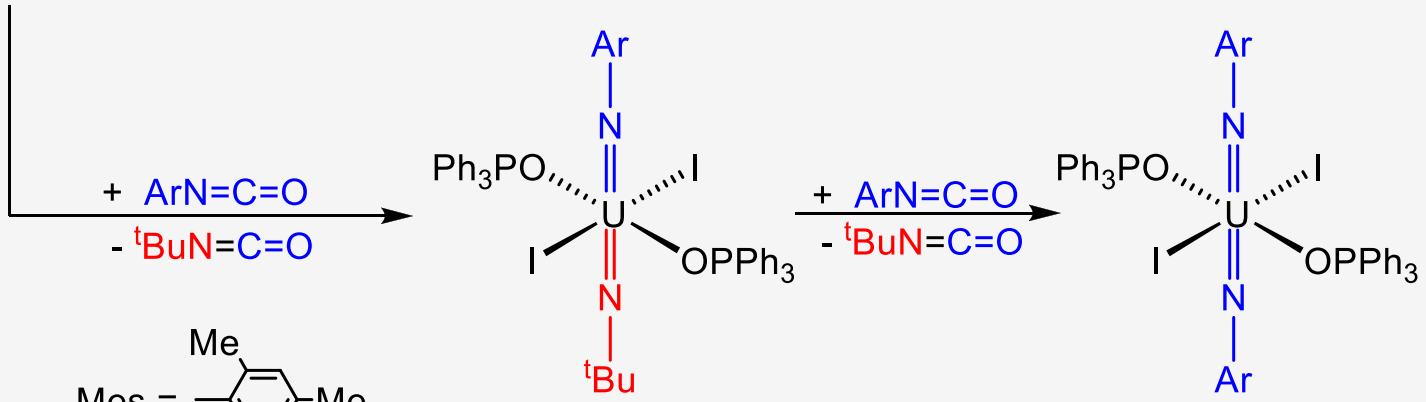

Mes = 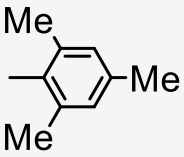

Ar = Ph (**3**); Mes (**4**)

Ar = Ph (**5**); Mes (**6**)

Spencer, Yang, et al., *J. Am. Chem. Soc.* **2008**, *130:* 2930

Reaction Mechanism: Imido Exchange

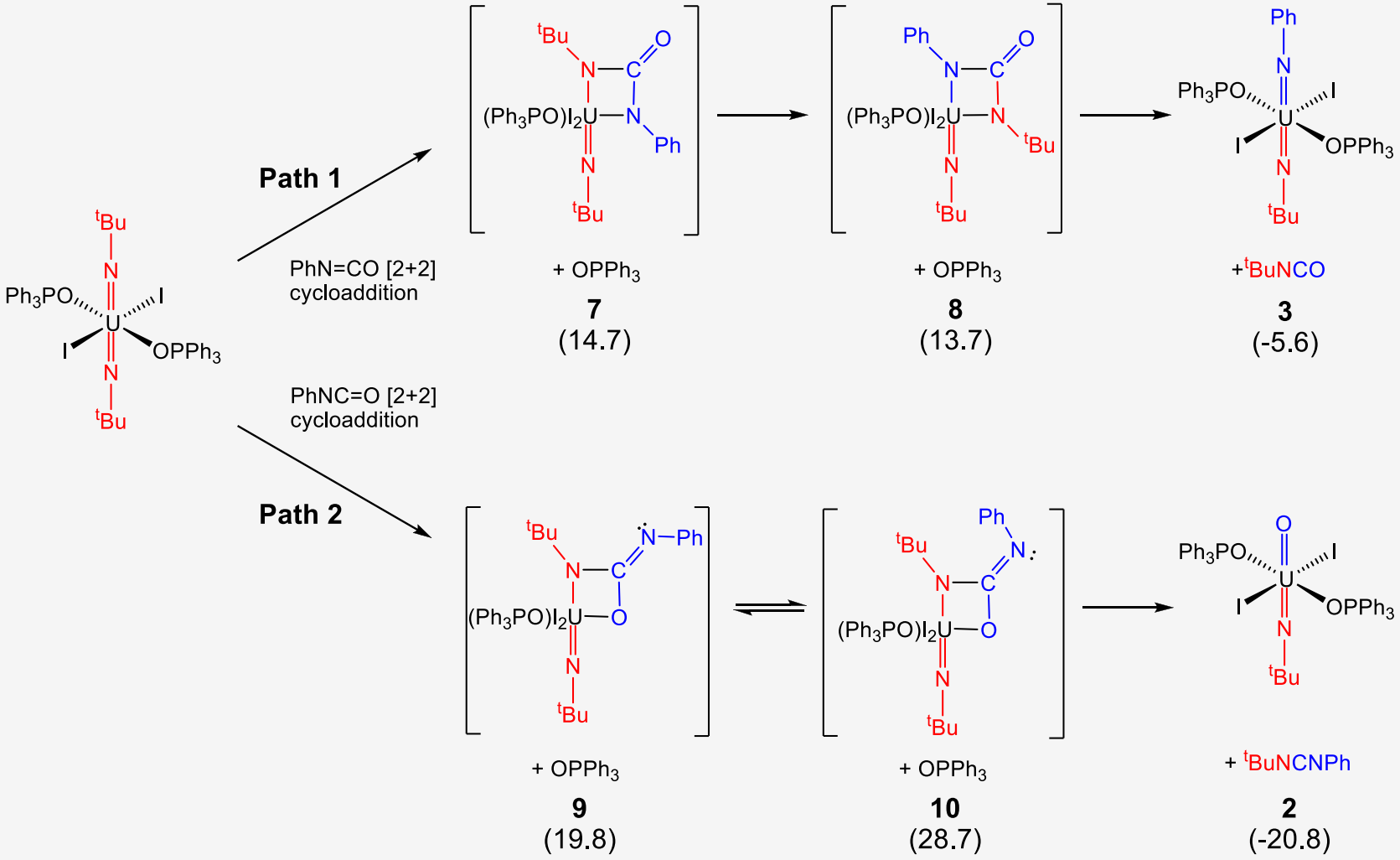

Spencer, Yang, et al., *J. Am. Chem. Soc.* **2008**, *130:* 2930